# Paleoenvironment and paleoclimate of the Late Cretaceous Ise Formation, Eastern Dahomey Basin.

**Adeoye Olugbemi Oshomoji** ( adeoye.oshomoji@oasisgeokonsult.com )
Oasisgeoconsulting Nigeria Limited

**Otobong Sunday Ndukwe**
Federal University Oye Ekiti, Ekiti State

**Kamaldeen O. L. Omosanya**
Oasisgeoconsulting Nigeria Limited

**M. A. Lawal**
Dr Moses Strauss Department of Marine Geosciences, Charney School of Marine Sciences, University of Haifa,

**Article**

**Keywords:** Cretaceous, Ise, Dahomey, sedimentology, palynomorphs, Climate, Vegetation

**Posted Date:** March 23rd, 2022

**DOI:** https://doi.org/10.21203/rs.3.rs-1453685/v1

# Abstract

The paleoenvironment and paleoclimate of the Ise Formation remain poorly understood, despite its importance for the Late Cretaceous paleoenvironment and geology of the Dahomey Basin and Africa in general. This is due to the paucity of outcrops and drilled samples of the formation. This study investigates the paleoenvironmental and paleoclimatic setting of the Ise Formation through sedimentological and palynological analyses of fifty sediment samples. The sediments were recovered from four exposed sections of the formation, three of which are recently exposed, in the Eastern Dahomey Basin, SW Nigeria. The examined sediments are largely coarse-grained, poorly sorted, gravelly-sand to sandy-gravels, and are dominated by spores and pollens. The Laevigatosporites sp. and the Sapotaceae sp. are the most abundant spores and pollens in the sediments while minor occurrences of Monocolpites sp., Cyathidites minor, Retitricolporites sp., and Spinizonocolpites sp. were recovered. Concentricytes sp. was the only algae recovered, while microforaminiferal wall lining was the only foraminifera recovered. Textural properties of the sediments indicate textural immaturity and proximity to the source area. The occurrence of Monocolite sp., Foveotriletes margaritae, Echitriporites trianguliforms, Cyathidites, and Longapertites sp. indicate a Maastrichtian to Early Paleocene age for the Ise Formation. The vegetation cover was mainly mangrove with palms, shrubs, and forests, while the environment of deposition was swamp to marginal nearshore. A dominant mild to warm tropical climate during the deposition of the formation was inferred based on the recovery of Retitricolporites sp., Monocolpites marginatus, Sapotaceae sp., and Spinozonocolpites sp. from the samples. These conclusions support the hypothesis of a regional shallow environment setting during the Maastrichtian and a warm regional climate in Africa during the Early Paleocene.


# 1. Introduction

The Ise Formation represents the oldest sedimentary sequence in the Dahomey Basin [1–5], yet its depositional settings and evolution remain poorly understood. Despite the fact that the basin has been widely studied, most previous studies on its eastern stretch i.e. Eastern Dahomey Basin in Nigeria, were focused on the geophysical properties [4,6]. Many also focused on partial biostratigraphic dating and sedimentologic descriptions of its sequences [1,7]. In particular, the overburden units comprising the Afowo and Ewekoro formations have received more attention mainly because of their significance for commercial exploration of oil sands, minerals, and limestone [2,5,8–10].

Current knowledge of the Ise Formation is limited to its sedimentologic characteristics [11,12], structural framework [3,13] and few biostratigraphic dating [5]. Till date, there is a general lack of understanding on the depositional settings, paleogeography, and climate of the formation. This is due mainly to the scarcity of outcrops and limited drilling in both onshore and offshore areas of the basin. Other causes include lack of detailed basin analysis studies and scanty dating of sediments within the basin. Like most Cretaceous rocks on the African continent, only a few outcrops of the Abeokuta Group, consisting of the Ise, Afowo, and Araromi Formations, are known [14,15]. Moreover, previous efforts to date the Ise Formation using

spores and pollen from an offshore exploration well failed because of the damaged nature of the recovered part of the formation (Kaki et al., 2012). Only the work of [2] based on one outcrop and samples analyzed from Onikintigbi, SW Nigeria show that the Ise Formation was deposited under an interplay of wet and dry climates. [5] also assigned an Early Cretaceous (Neocomian) age to the Ise Formation by counting sporomorphs, including Cicatricosisporites sp. Flora, recovered from the Ise-2 well drilled in the Nigerian section of the basin. Hence, it is imperative to investigate the paleoclimate and paleoenvironment of the formation.

In this work, a high-resolution sedimentological and palynological analyses of sediment samples recovered from four outcrops of the Ise Formation within the Eastern Dahomey Basin is performed. The outcrops include Onikintigbi-OK [2,9] and three others - Ojodu Berger (OB), Ijebu Ijesha (IJ), and Eregun (ER) that were only recently discovered due to excavation for road and building construction (Figure 1 and 2). To understand the environment and climate prevalent during the deposition of the Ise Formation, we carried out a detailed lithological description of the four rock exposures. We also analyzed 50 samples recovered across different lithologic facies on the exposures, for their provenance and palynomorph content. The sampled rocks were subjected to paleoenvironmental and paleoclimate analyses by relying on the abundance of palynomorphs. Palynomorphs are environmentally sensitive and proven markers of past environmental variables that controlled their distribution [16,17]. Thus, the methods and analyses presented in this work allowed the age, climate, vegetation, and environment of the Ise Formation to be reconstructed. The new knowledge presented in this work has wider implications for future research and for reappraising extant theories on the evolution of the Ise Formation and other regional Cretaceous sequences in Africa.

# 2. Geologic Setting And Lithostratigraphy Of The Abeokuta Group

The Dahomey Basin developed as a marginal pull-apart basin following the separation of the African and South American plates in the Mesozoic [5,18]. Tectonic evolution of the basin in the Late Jurassic to Early Cretaceous was characterized by both block and transform faulting when the African, North American, and South American paleocontinents separated [5,19]. The Dahomey Basin (Figure 1b and 3) consists of offshore, coastal, and inland parts, stretching from the southeastern part of Ghana in the west, through Togo and the Republic of Benin to the southwestern part of Nigeria in the east [18,20]. The portion of the basin that extends into Nigeria is popularly referred to as the Eastern Dahomey Basin. In this part, the Dahomey Basin is separated from one of the world's most prolific hydrocarbon province, the Niger Delta, by the Okitipupa Ridge, which is a faulted basement high [21,22].

Based on analysis of seismic and borehole data in offshore areas of the basin [3], the tectono-sedimentary evolution of the entire Dahomey Basin can be grouped into four stages. These are the pre-rift (up to Late Jurassic), syn-rift (Neocomian to Lower Cretaceous), transitional (Cenomanian to Santonian) and post-rift (Maastrichtian to Holocene) stages. These stages are also referred to as intracratonic, rift, transitional and drift stages; respectively [23–25]. In terms of basin infill, the oldest group of sediments in the Eastern

Dahomey Basin include the Cretaceous siliciclastics of the Abeokuta Group that lie unconformably on the crystalline basement rocks of Nigeria (Figures 3 and 4). The Abeokuta Group is further sub-divided based on lithologic heterogeneity and origin into the Ise, the Afowo, and the Araromi Formations from the oldest to the youngest [5,26]. Some of the formations, especially the Afowo, have been studied in few rock exposures in the southwestern part of Nigeria [7,9,20,27]. The Ise, Afowo, and Araromi Formations make up the Dahomey basin's thickest strata, reaching up to 2.5 km in the eastern part of the basin. In this part, the Abeokuta Group is overlain by Paleogene and Neogene strata of the Ewekoro, Akinbo, Oshosun, Ilaro and Benin formations [10,18].

The Ise Formation consists of imbricated basal conglomerates that are overlain by coarse to medium-grained sandstone with interbeds of kaolinite. Limestones are also known to occur within the formation at some locations [28]. Based on paleontological assemblages, a Neocomian-Albian is assigned to the Ise Formation [2]. Overlying the Ise Formation is the Afowo Formation, which consists of coarse- to medium-grained sandstones, thick interbedded shale, siltstone, and claystone. The sandstones are tar-bearing [9,29] while the shale is rich in organic matter [29]. A Turonian age is assigned to the lower part of the Afowo Formation, while the upper part is dated Maastrichtian [29]. The youngest formation in the Abeokuta Group is the Araromi Formation that is composed of fine- to medium-grained sandstones at the base. The sandstones are in turn overlain by shales, siltstone with interbedded limestone, marl, and lignite. Based on fauna content, the Araromi Formation is dated Maastrichtian to Paleocene [5].

# 3. Materials And Methods

The approach used in this work includes (a) detailed geological field mapping (b) laboratory analyses consisting of granulometric/grain size and palynological analyses.

### *Field mapping and sampling*

Detailed geological mapping was done at four rock exposures of the Ise Formation in Southwestern Nigerian (Figure 2). The field locations include OB in Lagos State, Nigeria, IJ, ER and OK (in the Omo Forest Reserve), all within Ogun State, also in southwestern Nigeria. At the outcrop locations, emphasis was given to (a) lithological logging of the outcrop (b) sample collection (c) overall description of the outcrops including topography, structures, and vegetation. Lithological logs were made at a high-resolution horizontal scale of 1: 200 cm and vertical scale of 1:250 cm. Three points were logged at each outcrop, including OB1, OB2, and OB3 at OB, IJ1, IJ2, and IJ3 at IJ, ER1, ER2 and ER3 at ER, and OK1, OK2 and OK3 at OK. The logs were described based on colour, lithology, grain size, roundness, and sedimentary structures. Variations in outcrop properties were logged individually at all outcrop locations and correlated across the four case study areas. Overall, 50 sediment samples were collected systematically at intervals of 0.25 m at OK and ER, and at intervals of 1 m at IJ and OB. Following field mapping and sample collection, the samples were air-dried at room temperature of $22^0$C for 7 days before being packed into transparent sample bags in preparation for laboratory analyses.

### *Granulometric analysis*

The grain size distribution for the samples was determined using 11 sieve meshes of different sizes (2 mm, 1.4 mm, 1 mm, 0.5 mm, 0.35 mm, 0.25 mm, 0.18 mm, 0.125 mm, 0.09 mm, 0.075 mm, and 0.063 mm) and a mechanical sieve shaker. The samples were pulverized and poured into the largest sieve (2 mm), then sieved mechanically for 15 minutes. During agitation, each sieve retains sediments that are larger than the mesh size. The sieves are then weighed to determine the amount of sediment retained. To understand the transportation and depositional history of the analyzed sediments, the grain size distribution for each sample and locations were analysed in Gradistat 8.0 [30] for the mean grain size, skewness, standard deviation (sorting), and kurtosis [31]. Each parameter was calculated using equations 1-4 below and were then classified based on the scheme of [31].

The graphical mean (φ) is the average size of grains within a sample [32,33]. The mean of sediments can be used to determine the energy conditions of transportation, as well as the distance travelled from the source area. For example, grain size decreases away from the source area, with the energy of transportation also decreasing away from the source area, and vice-versa [34]. Standard deviation (φ) is the measure of sorting or the spread of grain size distribution based on density [32,34]. Sorting indicates the deposition mechanism and energy conditions of the transporting medium. The sediments deposited quickly or under fluctuating transporting energy, tend to generally be poorly sorted. Sediments transported over a longer time, or with constant energy of transport, such as reworked sediments, beach and aeolian deposits generally have better sorting [34]. Skewness is the measure of symmetry of the grain size distribution [34]. The distribution can be fine or positively skewed, when there is an excess of fine particles. It can also be coarse or negatively skewed when the distribution is in excess of coarse-grained materials. For symmetrical grain size distribution, the skewness is zero [31–33]. Skewness reflects the deposition process. For instance, beach sediments tend to be negative or coarse skewed because of fine sediments being removed during continuous-wave actions. River sediments are positive or fine skewed because the finer particles are retained during transport and deposition [34]. Kurtosis reflects the degree of grain size distribution, where sharp peak curves (very leptokurtic and leptokurtic) reflect better sorting in the central portion of the distribution. Flat peak curves (platykurtic and very platykurtic) are suggestive of poor sorting [31–33].

$$M = \frac{\phi_{16} + \phi_{50} + \phi_{84}}{3} \quad \text{..... (1)}$$

$$Sk = \frac{\phi_{16} + \phi_{84} - 2\phi_{50}}{2(\phi_{84} - \phi_{10})} + \frac{\phi_5 + \phi_{95} - 2\phi_{50}}{2(\phi_{95} - \phi_5)} \quad \text{..... (2)}$$

$$K = \frac{\phi_{95} - \phi_5}{2.44(\phi_{75} - \phi_{25})} \quad \text{..... (3)}$$

$$SD = \frac{\phi_{84} - \phi_{16} - 2\phi_{50}}{4} + \frac{\phi_{95} - \phi_5}{6.6} \quad \text{..... (4)}$$

where M = mean, SK = skewness, SD= standard deviation, and K = kurtosis

Further analysis involved creating bivariate plots of the textural parameters listed above to establish empirical relationships between them. Correlation between these parameters have been shown to exist and reflect differences in sediment transportation and deposition patterns [35]. Bivariate analysis was performed for sediments from outcrops ER, IJ, OB, and OK to understand their depositional setting and transportation history. Accordingly, bivariate analysis was performed for skewness versus mean size, standard deviation versus mean, skewness versus standard deviation, kurtosis versus skewness, and kurtosis versus mean size.

### *Palynological analysis*

The procedure for the palynological analysis includes initial sample preparation and subsequent studies under the microscope. Samples were macerated with dilute Hydrochloric acid to remove any carbonaceous material (usually calcite) present in them. Rocks containing calcium carbonate generally effervesce in the presence of HCl acid. To digest the treated samples and remove siliceous matter, 60% Hydrofluoric acid (HF) was added to them as a supernatant liquid. As a result, the samples were soaked overnight and stirred intermittently with a plastic rod to achieve maximum digestion. Afterwards, the HF was decanted gently, and the remaining substrates were rinsed with distilled water. The samples were then sieved through the 5-10µ sieve to remove their clay and silt contents. Drops of nitric acid ($HNO_3$) were put in the residues to bleach them and further remove any remaining silt and clay. Potassium Hydroxide (KOH) was added to stop any oxidation reaction with $HNO_3$. To achieve heavy liquid separation, Zinc chloride ($ZnCl_2$) was added to different test tubes containing the residues. The residues were measured to the same level in the set and later placed in the centrifuge.

To ensure good separation of the samples, the centrifuge was operated at a revolution of 2000 per minute for 15 minutes. This allowed organic matter with specific gravity of less than 2.2 $gcc^{-1}$ (i.e., palynomorphs) to float while those heavier than 2.2 $gcc^{-1}$ settled to the bottom of the tube. The floated materials were carefully decanted into a clean tube and later rinsed with distilled water. In a final stage of treatment, the residues were rinsed with ethanol before being mounted on the slides. This was done to

achieve permanent slide preparation as the ethanol will remove any water trapped within the organic residue. The final slides were prepared by placing the residues rinsed with the ethanol on a covered slip that was in turn placed on a hot plate. Here, the residues are spread out and allowed to dry up. On the glass slide, drops of mountant liquid were added and spread instantly to cover the slip. The final slides were dried for ca. 2days and were studied under the microscope to identify pollen, spores, dinoflagellates, and freshwater algae.

# 4. Results

### 4.1 Lithologic description from outcrop observations.

The four (4) outcrops investigated were logged stratigraphically at 3 points each and described in terms of their lithology types, grain size, colour, fossil content, and sedimentary structures. Outcrops ER, IJ, and OB are road cut exposures while OK is a low-lying outcrop surrounded by dense vegetation (Figures 3 and 4).

### Outcrop OB (Figure 4a)

Outcrop OB is covered by sparse vegetation and has an altitude of 53 m above sea level. It is a road cut section with a vertical extent of ca. 8.2 m, length of ca. 30 m and strike in the SW-NE direction. Heights of points OB1, OB2, and OB3 at the outcrop location are 8.2 m, 7.8 m, and 4.8 m (Figures 4a and 6). The basal unit at OB1 is characterized by brownish-yellow sandstone (Figure 5d) and with clasts that are generally rounded and medium- to coarse- grained (Figure 4a, 5a and 6). The clasts become finer upwards as well as the clay content up till about 3.7 m where angular to subangular clasts are observed (Figure 5b). At the top of the section, the color of the sandstone changes to brown grey. The uppermost unit of the outcrop at this point is lateritic (Figure 6). Clayey-sandstone is observed as the basal unit at point OB2, albeit the sandstones are light brown-whitish grey, and with rounded, fine- to medium- grained clasts. The middle/intermediate units are quite like those of OB1 (Figure 6) while the uppermost unit is also reddish-brown laterite (Figure 6). Clayey sandstones with sub-angular clasts were also identified at the base of OB3 (Figure 5c). Here, the clasts are medium- to coarse- grained, white to light brown in color (Figure 5e), and their shape changes from rounded in the middle of the section (Figure 6) to sub-rounded towards the top (Figure 6).

### Outcrop IJ (Figure 4c and d)

The outcrop has an altitude of 85 m above sea level and length of ca. 60 m. Heights of the log points IJ1, IJ2, IJ3 are 7.8 m, 6.4 m, and 5.3 m respectively (Figure 4 c, d and 6). The surface of the outcrop is heavily scrapped due to sand quarrying in the area. At point IJ1, the outcrop grades from medium- to coarse-grained, reddish-brown sandstone with sub-angular clasts at the base to coarse to very coarse-grained, greyish-brown sandstone in the middle (Figures 4c and d). At the top of the outcrop at point IJ1, reddish-brown to grey, medium-grained sandstone with sub-rounded clasts are present (Figure 5i). The reddish color is attributed to increasing laterite content from base to top (Figure 5f). The stratigraphy at points IJ2

and IJ3 are quite like those at IJ1 in terms of color and texture. The base of the exposure at IJ2 is characterized by greyish-brown sandstone of medium- to very coarse texture and sub-angular clasts (Figure 6). The sandstone becomes a little clayey at a depth of 1.7 to 4.1 m, while the upper sections show brown, yellow to red-purple color (Figure 6). The sand clasts are very coarse-grained and with inclusion of well-rounded pebbles (Figure 6). The base of the section at IJ3 is made up of coarse-grained sandstone with angular clasts, while the top is characterized by brownish grey, coarse-grained sandstone, with sub-angular clasts and laterite (Figure 5g).

### Outcrop ER (Figures 4b)

Outcrop ER has a length of ca. 30 m and a vertical extent of 1.93 m, 1.21 m, and 1.07 m at points ER1, ER2, and ER3, respectively (Figure 7). Additionally, a thin layer comprising cobbles with diameters of 64 mm to 210 mm is observed. This is a paraconformity that is inclined at about $2^0$ to the south (Figure 4b). From base to top, point ER1 consists of grey to yellowish-brown, medium to very coarse-grained sandstones with sub-angular to well-rounded clasts (Figures 5h and 7). They become coarser upward until about 1.5m where the cobble-paraconformity is present. The cobbles are generally ferruginous in nature as indicated by their reddish-brown color. At the uppermost section, the sandstone becomes yellowish-brown and grey but with more sub-angular clasts (Figure 5h). The same stratigraphy is observed at the other two logging points: ER2 and ER3.

### Outcrop OK (Figure 4e and f)

Outcrop OK is a low-lying outcrop that extends laterally for ca. 15 m. Heights at log points OK1, OK2 and OK3 are 1.4 m, 1.23 m, 1.55 m, respectively. The strata at the base of the outcrop non-conformably overlie the weathered basement rock. Tabular crossbedding was also observed within the outcrop (Figures 4e, 4f and 7). The basal unit across OK1-OK3 is a weathered basement rock composed of kaolinite (Figure 4e and 4f). Clasts within the weathered unit are weathered feldspathic minerals that are suggestive of a granitic protolith. Above the basement lies grey to red, medium to coarse-grained sandstone with sub-rounded clasts (Figures 4e and 4f). The overlying sandstone is slightly muddy and light brown in colour and with clasts of white pebbles. At about 0.84 m to 1.16 m in the upper part of the section, the sandstone becomes conglomeratic although the texture remains the same as that of the older underlying sandstones (Figure 4e and 4f). The uppermost sandstone unit is brownish to white and coarse-grained with quartz pebble clasts ranging from 15 to 20 mm in diameter. Similar observations were made at points OK2 and OK3, except that the size of the quartz granules at about 0.3 to 0.7 m at OK2 ranges from 2.0 mm to 3.5 mm (Figure 7).

### 4.2 Sediment characterization and grain size parameters

The grain size ternary plot for the sediments from outcrops IJ, OB, OK, and ER is presented in Figure 8. Sediment samples from ER are classified as sandy gravel, those from OB plotted as slightly gravelly, gravelly sand to sandy gravel, while sediments from outcrops OK and IJ are sandy gravel and gravelly sand. Importantly, the calculated graphical Mean (Mz) ranges from -0.42 to 0.43 for IJ, 0.08 to 1.17 for

OB, -0.86 to -0.27 for ER, and 0.22 to 0.84 for OK (Figure 9). Hence, the average grain size is 0.05 for IJ and 0.66 for OB, signifying the predominance of coarse-grained sediments. The average grain sizes of sediments from ER and OK are -0.66 and -0.17 reflecting the predominance of very coarse-grained sediments. Similarly, the standard deviation for outcrops IJ, OB, ER, OK (Figure 10a) ranges from 1.07 to 1.37, 1.27 to 1.52, 0.69 to 1.21, and 0.65 to 1.22 while graphic skewness (Sk) ranges from 0.60 to 0.79 for ER, 0.08 to 0.36 for OB, 0.13 to 0.65 for IJ, and -0.02 to 0.60 for OK (Figure 10b). Most of the samples from OK fall predominantly within the very fine skewed class, with only 4 samples having a nearly symmetrical skewness. The samples from ER are very finely skewed, while those from IJ have fine to very-fine skewness. Samples from OB predominantly fall within the finely skewed class, with 5 samples being nearly symmetrical (Figure 10b). Kurtosis for IJ, OB, ER and OK sediments are from 0.73 to 1.03, 0.73 to 0.99, 0.83 to 2.30, and 0.79 to 1.16, respectively. These values indicate predominantly platykurtic-mesokurtic, predominantly platykurtic–mesokurtic, mesokurtic–very leptokurtic), and predominantly platykurtic distribution, respectively (Figure 10c). Based on the kurtosis, sediments from outcrops OK, IJ, and OB are characterized as being poorly sorted those of outcrop ER are moderately sorted.

In addition to the calculation of the statistical parameters, bivariate plots are shown in Figures 9 to 11b. The plot of skewness versus mean size shows that the Ise Formation samples are symmetrical to very fine skewed, albeit the samples are predominantly very fine skewed (Figure 9). Grain size ranges from medium to very coarse, with the coarse to very coarse sediments dominating the distribution. The environment of deposition corresponding to various classes of correlation of skewness against mean size are plotted in reference to various authors [35–37]. Accordingly, the samples plotted in the field of river processes and are classified as massive sandstones (Figure 9). The plots of standard deviation against mean size, and skewness against standard deviation reveal samples from the study area are moderately well sorted to poorly sorted, with the poorly sorted samples dominating the distribution. In terms of depositional setting, these bivariate plots (Figure 10a) show the influence of a riverine environment [35]. The sediments are also observed to be dominantly poorly sorted and show a fine to very skewed distribution (Figure 10b). Furthermore, the plots of kurtosis versus skewness, and kurtosis versus mean size show the samples are platykurtic to very leptokurtic but are mainly platykurtic and are symmetrical to very fine skewed. The very finely skewed class dominate the distribution (Figures 10c and 11b). A predominant riverine depositional setting is associated with virtually all the sediments from OK, OB, IJ and a few sediments from ER, while a beach setting is attributed to majority of the sediments from outcrop ER (Figure 10c).

### 4.3 Provenance of sediments based of grain size analysis

The statistical parameters presented above have different interpretations in relation to provenance or sediment source area. Sorting reflects the distance the sediments have travelled from the source [34]. The mean of sediments can indicate the depositional setting [32,34], while skewness and kurtosis can point to the difference in kinetic energy of the transporting medium [31,34]. Based on the average mean grain sizes of 0.05 φ for IJ, 0.66 φ for OB (coarse grained), -0.66 φ for ER, and -0.17 for OK (very coarse grained), and

the predominately fine and very fine skewness, the analyzed sediments have been transported and deposited under a fluvial depositional setting, with fluctuating energy [33,34]. Poorly sorted sediments at outcrops OK, IJ and OB, indicate deposition of the sediments near their source areas [32,34]. The dominance of moderately sorted sands, as well as very leptokurtic kurtosis of sediments at outcrop ER, suggests that the ER sediments achieved their sorting in a different high energy environment [31].

# 5. Occurrence And Distribution Of Palynomorphs In Sediments Across The Study Area

The occurrence and distribution of palynomorphs in sediments recovered from the study area is presented in Figures 12a and b, and Table 1. Laevigatosporites sp. (Figures 13 a and b) is the most abundant spores (n=8) in the study area, with the most recovery made at ER (n=4) followed by OK (n=2). Fungal spores are the second most abundant (n=6) and were observed at OB (n=3), OK (n=2), and IJ (1), respectively. Cyathidites sp. (n=5) (Figure 13h) was also found in three of the locations i.e., OB (n=1), ER (n=2), and IJ (n=2). Other identified spores include Cyathidites minor (Figure 13g); Foveotriletes margaritae (Figure 13c); Verrucatosporites sp. (Figure 13n); Trilete spore (Figure 13m); Acrostichum aureum (Figure 13f) and Spore indeterminate. As for the pollens, Sapotaceae sp. (Figure 13l) is the most abundant pollen (n=3) and was recovered at OK (n=2) and IJ (n=1). Monocolpites sp. was observed at both OB and IJ (Figure 14, Table 1), while Echitriporites trianguliforms (Figure 13o) was found at ER and IJ. Monocolpites marginatus (Figure 13i) was found at only ER and IJ (Figure 13). Other pollens recovered from the samples in the study area are Psilatricolporites sp. (Figure 13k), Longapertites sp. (Figure 13e), Retitricolporites sp. (Figure 13q), Spinizonocolpites sp. (Figure 13r). Concentricytes sp. is the only algae recovered from the samples and it was observed in OB (Figure 13p). Microforaminiferal wall lining (Figure 13d) was the only foraminifera recovered in the samples, precisely at ER. In summary, spores were relatively abundant in OB (73%) than the other palynomorphs, pollen (18%) and algae (9%) (Figure 14). They were also more abundant at ER (67%) than the pollen (25%) and foraminifera (5%).

### 5.1 Interpretation of age and Paleoenvironment from palynomorphs assemblages

#### *OB 1, 2 and 3*

Palynomorphs recovered from OB samples include Monocolpites sp. and Cyathidites (Figures 13, 14 and Table 1). The presence of Monocolpite sp. (Figure 14), indicate an age of Upper Maastrichtian to Early Paleocene [38], while Cyathidites signify an open freshwater swamp environment of deposition [39]. Fungal spores are observed in all the three logs at OB, and their presence also signifies that the sediments were deposited under swampy conditions [40]. Importantly, Concentricytes sp., which are freshwater alga [41] were identified at OB2 (Table 1), while Acrostichum aureum and Laevigatosporites were observed for OB1 samples. The occurrence of Acrostichum aureum and Laevigatosporites, which are land-derived species, in the samples indicates brackish conditions of sedimentation [42]. Laevigatosporites could also be linked to a swampy fresh water or brackish water environment [42].

### *ER 1, 2 and 3*

Palynomorph species recovered from the samples for ER 1, 2, and 3 include Monocolpite marginatus, Foveotriletes margaritae, Cyathidites sp., Echitriporites trianguliforms, Psilatricolporites sp., Verrucatosporite sp., and Laevigatosporite sp. (Figures 13, 14, and Table 1). The recovery of Monocolpites marginatus is indicative of wet mangrove to marsh vegetation with a predominantly warm and humid climate [43,44]. Monocolpites marginatus could also suggest deposition in a fluviatile environment [45]. The occurrence of Cyathidites sp in the samples indicates an open freshwater swamp environment of deposition [46]. Laevigatosporite sp. and Verrucatosporite sp. are indicative of swampy fresh or brackish water environment [42]. Verrucatosporites are traditionally associated with deposition in brackish water environment during a sea-level rise [47]. Microforaminiferal test lining was observed from ER sediments (Table 1). Their occurrence indicates proximity to marginal marine setting, notably a nearshore environment [48]. Other palynomorphs recovered from the ER samples are Foveotriletes margaritae and Echitriporites trianguliforms, which are suggestive of a Maastrichtian to Paleocene age [49,50]. The occurrence of Echitriporites trianguliforms also indicate that the sediments were deposited in near shore settings.

### *IJ 1, 2 and 3*

Pollen and spores recorded from IJ samples include Fungal spore, Trilete spore, Monocolpite marginatus, Cyathidites minor, Cyathidites sp., Foveotriletes margaritae at IJ1 (Figure 13, 14 and Table 1). Echitriporites trianguliforms and Monocolpites sp. at IJ 2 and Acrostichum aureum, Longapertites sp., Sapotaceae and Cyathidites sp. at IJE 3 (Figures 13, 14 and Table 1). The occurrence of Cyathidites sp. here supports open freshwater swamp environment of deposition [39]. The sediments contain a single record of Microforaminiferal wall lining, but without the occurrence or evidence of dinoflagellate cysts. Hence, the samples were interpreted to be deposited in near shore settings [51]. The presence of Longapertites sp. in the samples suggests wet mangrove to marsh vegetation under a warm and humid climate and an Early Maastrichtian age [52,53]. Cyathidites minor indicates upper Paleocene boundary [54]. The occurrence of Sapotaceae could be used to infer a freshwater swamp rainforest environment [55] ,while the presence of Retitricolporites sp. suggest mild to warm and temperate to subtropical climate in a lowland setting [56].

### *OK 1, 2 and 3*

At OK, Spinizonocolpites sp., Longapertites sp., Sapotaceae, Verrucatosporites sp., Laevigatosporite sp., Cyathidites minor, and fungal spore were recovered (Figures 13, 14 and Table 1). Spinizonocolpites sp. in the sample suggests a warm, humid, or tropical environment of deposition [57]. Additionally, fungal spore was recorded in OK 1 and OK 3. Sapotaceae, which is a land-derived specie [58] occurs within the study area. In the samples at OK 3, both the Laevigatosporite sp. and Verrucatosporite are observed, pointing to a swampy fresh water or brackish water environment [42]. There was no record of dinoflagellate cysts or

Microforaminiferal wall lining at OK 1-3. Hence, the sediments at OK1-3 are interpreted to have been deposited in a coastal deltaic environment. The age of the outcrop is dated Upper Maastrichtian to Early Paleocene age based on the occurrence of Longapertites sp. [59].

# 6. Late Cretaceous Climate, Vegetation, And Environment Of Deposition In The Study Area.

The climate, vegetation, and environment prevalent during the deposition of the Ise Formation are barely documented. Like other Cretaceous strata in Africa, extreme scarcity of exposed rocks has hindered research on the Cretaceous climate record of the Ise Formation and those of other similar formations on the continent of Africa relative to their surrounding landmasses [14]. Based on the analyses of palynomorphs from four rock exposures in the Eastern Dahomey, we show that the dominant climate during the deposition of the Ise Formation was mild to warm tropical climate. The vegetation cover was mainly mangrove with palms, shrubs, and forests, while the environment of deposition was swamp to marginal nearshore setting. Importantly, an average precipitation of at least 60 mm [60] is inferred, with modest seasonal variation in temperature and precipitation regimes [61] during the deposition of the Ise Formation.

Paleoclimatic indicators of tropical conditions in the study area are Retitricolporites sp. and Monocolpites marginatus at ER, Sapotaceae sp. at IJ, and Spinizonocolpites sp. at OK (Figures 13 and 14). Sapotaceae sp. at IJ significantly indicate swamp and tropical rainforest conditions [55], while Spinizonocolpites sp. at OK reflects warm and humid tropical environment [57]. Retitricolporites sp. and Monocolpites marginatus are palm pollen that are commonly found in contemporaneous West African coastal basins [46,62–64]. Sapotaceae is one of the latex-yielding families, known to produce Gutta percha, chicle (chewing) gum, timber, edible flowers, fruits, and oil seeds [58]. The plants of Sapotaceae are trees or shrubs, and the fruit is an indehiscent, one- to eight-seeded berry (sometimes a drupe). The seeds consists of crustaceous, shining testas, and are oily and ex-albuminous with large, fleshy cotyledons, or albuminous with flat cotyledons [58]. Spinizonocolpites sp. represents the earliest palm pollen known and are globally acknowledged as ancestral to the modern genus Nypa [65]. Spinizonocolpites sp. can include S. echinatus and S. baculatus [66,67], originally recovered from the Late Cretaceous of Sarawak [68]. The spiny zonasulcate pollen (Figure 13) is usually found as one half of the original spheroidal grain, due to breakdown of the aperture membrane during fossilization [65].

Paleo-vegetation fingerprints recovered from the samples include Monocolpites marginatus, Spinizonocolpites sp. and Longapertites sp. These are palynomorphs produced by plants adapted to the mangrove biome to marsh vegetation [43,44,49,69]. Monocolpites marginatus are common in coastal lowland forests or mangroves [49] where salt-tolerant trees (halophytes) grow in coastal saline or brackish water of tropical to subtropical climates [70]. Acrostichum aureum and Laevigatosporites at both OB and OK, and Verrucatosporite sp. at ER markedly indicate brackish water condition (Figure 13 and 14).

Acrostichum aureum is a large evergreen fern with fronds up to 3 meters long, and the plant is often harvested from the wild for local use as a food, material for thatching, and as an ornamental plant in gardens [71]. Acrostichum aureum are principal ferns currently growing within mangrove vegetation and are adapted to coastal areas associated with mangrove vegetation, areas inundated with saline waters, open salt marshes, coastal swamps, and areas along estuarine rivers [71]. Laevigatosporites on the other hand are monolete pteridophyte spores of ferns found in humid climate [72,73]. Therefore, the prevalent vegetation type in the Late Cretaceous of the study area was tropical mangrove.

Consequently, based on paleo-environmental markers such as Cyathidites, Concentricytes sp., microforaminiferal test lining, Echitriporites trianguliforms, Monocolpites marginatus, Spinizonocolpites sp., and Longapertites sp., a conceptual diagram showing the dominant environment of deposition in the study area is provided in Figure 15a. Cyathidites and Concentricytes sp., recovered at OB and IJ suggests an open freshwater environment of deposition, while fungal spores at the same location favors deposition under swampy conditions [41,73]. Deposition under nearshore environment is indicated by the presence of microforaminiferal test lining [48] and Echitriporites trianguliforms at ER, while marginal marine condition under the influence of rivers is indicated by Monocolpites marginatus [45] also at ER (Figure 14). Cyathidites are pteridophyte spores from evergreen and broadleaf trees found in humid climates [72]. Echitriporites trianguliforms are proteaceae i.e., family of shrubs and trees, while Concentricytes sp. are indicative of dominant fluvial system or shallow environment proximal to shorelines [41,73]. Palynomorphs such as Spinizonocolpites sp. and Longapertites sp. also support a continental environment of deposition [52,53].

The conceptual model shows that the study area was in an open marine environment in the Late Cretaceous. Sediments were transported from the continent or land areas by rivers and channels, and deposited in a delta at OK, while sediment deposition at OB, ER, and IJ were under swampy conditions. Based on this interpretation, sandstones in OK are interpreted to include mainly deltaic sands. Moreover, the recovery of Acrostichum aureum, Laevigatosporites and Sapotaceae in some of the sediments indicates land-derived species [42]. This is also corroborated by the grain size analyses result, which shows the sediments these outcrop locations are very coarse grained, poorly sorted, gravelly sand to sandy gravels (Figures 8 and 9), signifying their relative short transport distance, textural immaturity, and proximity to their source areas.

### 6.1 Age of the Ise strata.

Apart from the challenge of finding rock exposures of the Ise Formation in the Dahomey Basin, the few studies that described the stratigraphy of the basin have been quite limited in terms of data coverage. Despite being the oldest (pre-rift) strata of the Dahomey Basin [25,74,75], most previous descriptions of the Ise Formation were largely done from few boreholes and seismic reflection data. For example, the age of the Ise Formation was roughly put at Neocomian, probably Valanginian-Barremian by [5]. These authors based their dating on the recovery of sporomorphs such as Cicatricosisporites sp., pilosisporites,

trichopapillosus from the Ise-2 borehole. The biostratigrahic dating provided by [5] has been used for most referenced work on the age of the Ise Formation [13,26]. Moreover, in offshore areas, the age of the Ise Formation has been put at Neocomian [24], implying that the strata were pre-rift or deposited prior to the opening of the Equatorial Atlantic.

In the Eastern Dahomey Basin in Nigeria, the thickness, age, and nature of the Ise Formation is also barely known. For example, [76] schematically show that the Upper Cretaceous and Cenozoic rocks comprising the Ise Formation and younger rocks are barely exposed in the Eastern Dahomey Basin and are probably thinnest to the north or in onshore areas (Figure 1b). This thickness variation probably reflects (a) the tilted nature of the basin to the south (b) high preservation of the Ise strata in offshore areas, with thickness reaching up to 3 km in the Togo-Benin margin (Figure 1b), and (c) the presence of tilted basement blocks, grabens, and half grabens in offshore areas [24]. Regardless of these discrepancies in age, our study show that the Ise Formation is diachronous in onshore areas. Our estimated age is from the Upper Maastrichtian to the Paleocene (Figure 14). The presence of Monocolpite sp. at OB indicate an age of Upper Maastrichtian to Early Paleocene [38], Foveotriletes margaritae and Echitriporites trianguliforms at ER suggest Maastrichtian to Paleocene age [49,50]. Cyathidites at IJ delimit the upper Paleocene boundary, while Longapertites sp. at OK and IJ indicates Upper Maastrichtian-Early Paleocene age [59].

### 6.2 Evolution of the study area in the context of Albian breakup.

Based on the age markers presented in this work, we unequivocally put the age of the Ise Formation in onshore areas in Nigeria to be Maastrichtian and Early Paleocene and examine the interpreted environment of deposition within the context of the Albian breakup and the opening of the southern Atlantic Ocean. Previous works on the paleogeography of marginal basins along the southern Atlantic show that the Maastrichtian (72 to 66 Ma) was dominated by brief continental flooding and re-establishment of the Trans-Saharan Seaway [76]. A marine transgression during the Maastrichtian flooded West Africa briefly while marine sediments interbedded with brackish-water deposits are preserved east of the subsiding Hoggar shield (Figure 15b). During this period, the trans-Saharan seaway was probably re-established through the Bida rift [77], which began to form in the Campanian and continues to develop during the Maastrichtian under shallow-marine environment [78,79]. Accordingly, the study area, interpreted as an open marine environment from the palynomorph assemblages fits into a regional context of the shallow environment setting during the Maastrichtian. Moreover, [76] documented that marine transgression was also recorded on the Ivory Coast–Ghana and Ghana-Benin margin segments by the flooding of the coastal basins. From 72 to 66 Ma (Figure 15b), the environment of deposition therefore changed from marine to continental and is evidenced by (a) a mobile eastern shoreline of the trans-Saharan seaway that was associated with transient erosion at the Hoggar and Nigerian shield areas, (b) flooding of the Nigerian shield area, and part of the Saharan domain and (c) the establishment of large deltaic systems along the Central Atlantic coast, signifying drainage reorganization and/or upwarping of the margin [76]. The last phases of marine transgression were recorded in the Paleocene from 61 to 56 Ma

(Figure 15c), while the study area was still a coastal to open marine environment. Inland shoreline migration was reported along the Central and equatorial Atlantic margins, leading to deposition of marine limestones and shales in coastal basins [75]. Intense weathering caused by peak greenhouse climate allowed bauxites to develop in most basins [80]. In tandem, the interpreted climatic condition of warm tropical climate based on the recovery of Retitricolporites, Monocolpites marginatus, Sapotaceae sp., and Spinizonocolpites sp. from this study support the hypothesis of a warm regional climate in Africa during the Late Paleocene from 61 to 56 Ma (Figure 15c).

# 7. Conclusions

Outcrops of the Ise Fm. within the Eastern Dahomey Basin represent some of the few outcrops of Late Cretaceous rocks in Africa. Consequently, sedimentological and palynological analyses of sediments recovered from these outcrops provide ample opportunities to further understand the geology, paleoenvironment, and paleoclimate of Africa in the Cretaceous. Sedimentological analysis shows that sediments from the studied outcrops are generally texturally immature and are close to their source area, while palynological analysis indicates a Maastrichtian to Early Paleocene age for the Ise Formation based on the occurrence of index fossils. Palynological analysis also revealed that the vegetation during the deposition of the formation was mainly mangrove with palms, shrubs, and forest, while the paleoenvironment was swamp to marginal nearshore. The main climate type during this period was mild to warm tropical climate.

# Declarations

The authors declare that they have no known competing financial interests or personal relationships that could have appeared to influence the work reported in this paper.


### Funding

This project was independent research, was not funded and has not received funding from any organization or government


**Conflicts of interest/Competing interests (include appropriate disclosures):** The author declare that they have no known competing financial interests or personal relationships that could have appeared to influence the work reported in this paper.

**Availability of data and material (data transparency):** The data for the grain size analysis are provided here as supplementary data.

### Authors' contributions

**Oshomoji, Adeoye Olugbemi**- Coordination, Administration, Field work, Grain size analysis, Writing, Review, and validation.

**Ndukwe, Otobong Sunday**- Palynological analysis, Writing, Tables, Figures, and Review.

**Omosanya, Kamaldeen O. L**- Conceptualization, Administration, Writing, Figures, Review, and validation.

**Lawal, M. A**- Administration, Writing, Review, and validation.

# References


1. Adekeye, O. A., Gebhardt, H., Akande, S. O., Adeoye, J. A. & Abdulkadir, I. A. Biostratigraphic Analysis of the Cretaceous Abeokuta Group in the Eastern Dahomey Basin, Southwestern Nigeria. *Journal of African Earth Sciences* **152**, 171–183 (2019).
2. Akinmosin, A. A., Omosanya, K. O., Ikhane, P. R., Mosuro, G. O. & Adetoso, A. O. Electrical Resistivity Imaging (ERI) of basin fills in some parts of Eastern Dahomey. *International Research Journal Geology and Mining* **2**, 174–185 (2012).
3. Kaki, C., d'Almeida, G. a. F., Yalo, N. & Amelina, S. Geology and Petroleum Systems of the Offshore Benin Basin (Benin). *Oil Gas Sci. Technol. – Rev. IFP Energies nouvelles* **68**, 363–381 (2013).
4. Mosuro, G. O. *et al.* Redefining the boundary between crystalline and sedimentary rock of Eastern Dahomey Basin. *Sci Rep* **11**, 5016 (2021).
5. Omatsola, M. A. & Adegoke, O. S. Tectonic evolution and Cretaceous stratigraphy of the Dahomey Basin. *Journal Mining Geology* **18**, 130–137 (1981).
6. Okoro, E. M., Onuoha, K. M., Okeugo, C. G. & Dim, C. I. P. Structural interpretation of High-resolution aeromagnetic data over the Dahomey basin, Nigeria: implications for hydrocarbon prospectivity. *J Petrol Explor Prod Technol* **11**, 1545–1558 (2021).
7. Bolaji, T. A., Ndukwe, O. S., Oyebamiji, A. R. & Ikegwuonu, O. N. Palynological Age Control and Paleoenvironments of the Paleogene Strata in Eastern Dahomey Basin, Southwestern Nigeria. *Sci Rep* **10**, 8991 (2020).
8. Adegoke, O. S. *et al.* Tarsands—A new energy raw material in Nigeria. in *Proceeding of symposium on new energy raw material Karlovy vary* 17–22 (1981).
9. Eruteya, O. E. *et al.* Geoelectrical resistivity imaging of shallow oil sands in the Eastern Dahomey Basin (SW Nigeria): Implication for heavy oil exploration and production. *Journal of African Earth Sciences* 104122 (2021) doi:10.1016/j.jafrearsci.2021.104122.
10. Nton, M. E., Ikhane, P. R. & Tijani, M. N. Aspect of Rock-Eval Studies of the Maastrichtian-Eocene Sediments from Subsurface, in the Eastern Dahomey Basin Southwestern Nigeria. *European Journal of Scientific Research* **25**, 417–427 (2009).
11. MacGregor, D. S., Robinson, J. & Spear, G. Play fairways of the Gulf of Guinea transform margin. *Geological Society, London, Special Publications* **207**, 131–150 (2003).
12. Madukwe, H. Granulometric Analysis Of The Sandstone Facies Of The Ise Formation , Southwestern Nigeria. https://www.semanticscholar.org/paper/Granulometric-Analysis-Of-The-Sandstone-Facies-Of-%2C-Madukwe/3794b67203021c38cf02934c2df81176c1d09d53 (2016).

13. d'Almeida, G. A. F., Kaki, C. & Adeoye, J. A. Benin and Western Nigeria Offshore Basins: A Stratigraphic Nomenclature Comparison. *IJG* **07**, 177–188 (2016).
14. Orr, T. J. *et al.* Paleoclimate and paleoenvironment reconstruction of paleosols spanning the Lower to Upper Cretaceous from the Rukwa Rift Basin, Tanzania. *Palaeogeography, Palaeoclimatology, Palaeoecology* **577**, 110539 (2021).
15. Reyment, R. A. & Dingle, R. V. Palaeogeography of Africa during the Cretaceous Period. *Palaeogeography, Palaeoclimatology, Palaeoecology* **59**, 93–116 (1987).
16. Head, M. J. & Westphal, H. Palynology and paleoenvironments of a Pliocene carbonate platform: the Clino core, Bahamas. *J. Paleontol.* **73**, 1–25 (1999).
17. Morley, R. J. Palynological evidence for Tertiary plant dispersals in the SE Asian region in relation to plate tectonics and climate. *Biogeography and geological evolution of SE Asia* 211–234 (1998).
18. Whiteman, A. J. *Nigeria: Its Petroleum Geology, Resources and Potential*. vol. 2 (Grahan and Trontman, 1982).
19. Mascle, J., Blarez, E. & Marinho, M. The shallow structures of the Guinea and Ivory Coast-Ghana transform margins: Their bearing on the Equatorial Atlantic Mesozoic evolution. *Tectonophysics* **155**, 193–209 (1988).
20. Olabode, S. O. Siliciclastic slope deposits from the Cretaceous Abeokuta Group, Dahomey (Benin) Basin, southwestern Nigeria. *Journal of African Earth Sciences* **46**, 187–200 (2006).
21. Burke, K., Dessauvagie, T. F. J. & Whiteman, A. J. Opening of the Gulf of Guinea and geological history of the Benue Depression and Niger Delta. *Nature physical science* **233**, 51 (1971).
22. Obaje, N. G. *Geology and Mineral Resources of Nigeria*. vol. 120 (Springer Berlin Heidelberg, 2009).
23. Hessouh, M., Marcos, I., Pereira, J. J. & Farhangui, H. J. Hydrocarbon prospects for exploration and production. *Ministry of Energy, Mines, and Hydraulics, Republique du Benin* (1994).
24. Kaki, C., Oyede, L. M., Laibi, R. A. & Yessoufou, S. Influence de la dynamique sédimentaire et structurale sur la formation des réservoirs détritiques du Crétacé dans le bassin sédimentaire côtier (RESO-BSC) du Bénin (Golfe du Bénin, Afrique de l'Ouest),. in *Symposium sur la "redéfinition du socle du bassin sédimentaire côtier du Bénin"* 213–237 (Actes, 2001).
25. Tucker, J. W. Aspects of the Tano Basin stratigraphy Revealed by Recent Drill in Ghana. *Bulletin des Centres de Recherches Exploration-Production Elf-Aquitaine* **Memoire, 13,** 153–159 (1992).
26. Okosun, E. A. A review of the Cretaceous stratigraphy of the Dahomey Embayment, West Africa. *Cretaceous Research* **11**, 17–27 (1990).
27. Mohammed, S., Opuwari, M. & Titinchi, S. Source rock evaluation of Afowo clay type from the Eastern Dahomey Basin, Nigeria: insights from different measurements. *Sci Rep* **10**, 12036 (2020).
28. Nton, M. E. Sedimentological and geochemical studies of rock units in the eastern Dahomey Basin, southwestern Nigeria. (University of Ibadan, 2001).
29. Enu, E. I. Textural characteristics of the Nigerian tar sands. *Sedimentary Geology* **44**, 65–81 (1985).

30. Blott, S. J. & Pye, K. Gradistat: A Grain size distribution and statistics package for the analysis of unconsolidated sediments. *Earth Surface Processes and Landforms* 1237–1248 (2001).
31. Folk, R. L. & Ward, W. C. Brazos River bar: Astudy in the significance of grain size parameters. *Journal of Sedimentary Petrology* 3–6 (1957).
32. Boggs, S. *Principles of sedimentology and stratigraphy*. (Pearson Prentice Hall, 2006).
33. López, GI. Grain Size Analysis. in *Encyclopedia of Geoarchaeology* (ed. Gilbert, AS.) 341–348 (Springer Netherlands, 2017). doi:10.1007/978-1-4020-4409-0_18.
34. Tucker, M. E. *Sedimentary petrology: an introduction to the origin of sedimentary rocks*. (Blackwell Science, 2001).
35. Friedman, G. M. Dynamic Processes and Statistical Parameters Compared for Size Frequency Distribution of Beach and River Sands. *SEPM JSR* **Vol. 37**, (1967).
36. Moiola, R. J. & Weiser, D. Textural parameters: An evaluation. *J Sediment Petrol.* 45–53 (1968).
37. Stewart, H. Sedimentary reflection on depositional environment, in San Mignellagoon, Baju California, Mexico. AAPG Bull. 2567-2618. (1958).
38. Puri, G. S. in *Some plant microfossils from Nigeria Proceedings of the Central African Scientific and Medical Congress,Lusoka,N.Rhodesia,Aug.1963, Pergamon Press P* 391–404 (1965).
39. Brenner, G. J. Middle Cretaceous floral Provinces and Early migrations of angiosperms. in *Origin and Early Evolution of Angiosperms.C.B.Beck* (ed. editor) 23–47 (New York;Columbia University Press P, 1976).
40. Akpofure, E. & Akana, S., T. Palynomorphs assemblage and Paleoecology interpretation of Ajali sandstones in Western Anambra Basin of Nigeria. *J. Envt. and Earth Sci* **6**, 215–227 (2016).
41. Adeonipeku, P. A. & Olowokudejo, J. D. Palynology of Recent Bottom Sediments from Shallow Offshore Niger/Cross River Delta Nigeria: A Preliminary Study. *International J. of Botany* **9**, 100–122 (2013).
42. Asadu, A. N. & Chinemelu, E. S. Palynomorphs and Paleo-depositional environment of Well Z, OPL 310, Dahomey Basin, South-Western Nigeria. *Journal of Scientific and Engineering Research* **7**, 248–257 (2020).
43. Kogbe, C. A. Continental Terminal: in the Upper Benue Basin of North-Easter Nigeria Earth Evolution Sciences. (1981).
44. Lawal, O. Palynological biostratigraphy of Cretaceous sediments in the Upper Benue Basin, Northeast Nigeria. [ Biostratigraphie palynologique des sediments du Cretace dans le Bassin de la Haute-Benoue(Nigeria n.E. *] Revue de Micropal©ontologie* **29 # 1 P**, 61–83 (1986).
45. Adegoke, O. S., Agumanu, A. E., Benkhelil, M. J. & Ajayi, P. O. New stratigraphic, sedimentologic and structural data on the kerri-kerri formation, Bauchi and Borno States, Nigeria. *Journal of African Earth Sciences (1983)* **5**, 249–277 (1986).
46. Lawal, O. & Moullade, M. Palynological biostratigraphy of Cretaceous sediments in the Upper Benue Basin, N.E. Nigeria (1). *Revue de Micropaléontologie* **29**, 61–83 (1986).

47. Salard-Cheboldaeff, M. Palynologie maestrichtienne et tertiaire du cameroun. Resultats botaniques. *Review of Palaeobotany and Palynology* **32**, 401–439 (1981).
48. Concheyro, A., Caramés, A., Amenábar, C. R. & Lescano, M. Nannofossils, foraminifera and microforaminiferal linings in the Cenozoic diamictites of Cape Lamb, Vega Island, Antarctica. *Polish Polar Research* **35**, 1–26 (2014).
49. Germeraad, J. H., Hopping, C. A. & Muller, J. Palynology of tertiary sediments from tropical areas. *Review of Palaeobotany and Palynology* **6**, 189–348 (1968).
50. van Hoeken-Klinkenberg, P. M. J. Maastrichtian Paleocene and Eocene pollen and spores from Nigeria. *Leidse Geologische Mededelingen* **38**, 37–44 (1966).
51. Tyszka, J., Godos, K., Goleń, J. & Radmacher, W. Foraminiferal organic linings: Functional and phylogenetic challenges. *Earth Science Reviews* **220**, 103726 (2021).
52. Rull, V. Palaeofloristic and palaeovegetational changes across the Paleocene/Eocene boundary in northern South America. *Review of Palaeobotany and Palynology* **107**, 83–95 (1999).
53. Rull, V. Biogeographical and evolutionary considerations of Mauritia (Arecaceae), based on palynological evidence. *Review of Palaeobotany and Palynology* **100**, 109–122 (1998).
54. Igbinigie, N. S. & Akenzua-Adamczyk, A. H. Palynological studies of Maastrichtian to paleocene sediments exposed at Okpekpe, western flank of Anambra Basin, Edo State, Nigeria. *Journal of Applied Sciences and Environmental Management* **22**, 1563–1566 (2018).
55. Ola, P. S. & Adewale, B. K. Palynostratigraphy and paleoclimate of the sequences penetrated by Meren 31 side tract-2 well, offshore Niger delta. *International Journal of Geosciences* **5**, 1206 (2014).
56. Jarzen, D. M. & Klug, C. A preliminary investigation of a lower to middle Eocene palynoflora from Pine Island. *Palynology* **34**, 164–179 (2010).
57. Schrank, E. Organic-walled microfossils and sedimentary facies in the Abu Tartur Phosphates (Late Cretaceous, Egypt. *Berlin Geowiss* (1984).
58. Vaghani, S. N. FRUITS OF TROPICAL CLIMATES | Fruits of the Sapotaceae. in *Encyclopedia of Food Sciences and Nutrition (Second Edition)* (ed. Caballero, B.) 2790–2800 (Academic Press, 2003). doi:10.1016/B0-12-227055-X/00536-8.
59. Edet, J. J. & Nyong, E. E. Palynostratigraphy of Nkporo Shale exposures (Late Campanian-Maastrichtian) on the Calabar Flank, SE Nigeria. *Review of palaeobotany and palynology* **80**, 131–147 (1994).
60. McKnight, T. L. & Hess, D. *Physical geography: a landscape appreciation*. (Prentice Hall, 2000).
61. Kellman, M. & Tackaberry, R. *Tropical Environments*. (Routledge, 2003). doi:10.4324/9780203392843.
62. Durugbo, E. U. & Aroyewun, R. F. Palynology and paleoenvironments of the upper araromi Formation, Dahomey Basin, Nigeria. *Asian Journal of Earth Sciences* **5**, 50–62 (2012).
63. Eisawi, A. & Schrank, E. Terrestrial palynology and age assessment of the Gedaref Formation (eastern Sudan). *Journal of African Earth Sciences* **54**, 22–30 (2009).

64. Van Der Hammen, T. El desarrollo de la flora colombiana en los periodos geológicos. I. Maestrichtiano hasta Terciario más inferior. *Boletín Geológico* **2**, 49–106 (1954).
65. Harley, M. M. A summary of fossil records for Arecaceae. *Botan J Linn Soc* **151**, 39–67 (2006).
66. Hoorn, C. *et al.* A late Eocene palynological record of climate change and Tibetan Plateau uplift (Xining Basin, China). *Palaeogeography, Palaeoclimatology, Palaeoecology* **344–345**, 16–38 (2012).
67. Muller, J. Palynology of the Pedawan and Plateau Sandstone Formations (Cretaceous-Eocene) in Sarawak, Malaysia. *Micropaleontology* **14**, 1 (1968).
68. Morley, R. J. *Origin and evolution of tropical rain forests*. (Wiley, 2000).
69. Van Der Hammen, T. Climatic periodicity and evolution of South American Maastrichtian and Tertiary floras. *Boletín Geológico* **5**, 49–91 (1957).
70. Giri, C. *et al.* Status and distribution of mangrove forests of the world using earth observation satellite data. *Global Ecology and Biogeography* **20**, 154–159 (2011).
71. *Dictionary of gardening*. (Macmillan Press ; Stockton Press, 1992).
72. Bilobé, J. A., Feist-Burkhardt, S., Eyong, J. T. & Samankassou, E. Biostratigraphy of Cretaceous-Neogene sedimentary infill of the Mamfe basin, southwest Cameroon: Paleoclimate implication. *Journal of African Earth Sciences* **182**, 104279 (2021).
73. Mbesse, C. O. *et al.* Palynostratigraphy and paleoenvironmental reconstitution of the Paleocene-Eocene N'kapa Formation: Ngata and Moulongo series (Douala sub-basin, Cameroon). *Geobios* **69**, 37–53 (2021).
74. Billman, H. G. Palynology and Paleoenvironments of the Upper Araromi Formation, Dahomey Basin, Nigeria. in *Proceedings of the 7th African Micropaleontological Colloquium* 27–42 (1976). doi:10.3923/ajes.2012.50.62.
75. Brownfield, M. E. & Charpentier, R. Geology and total petroleum systems of the Gulf of Guinea Province of west Africa. *U.S Geological Survey Bulletin* **2207–C**, 32 (2006).
76. Ye, J. *et al.* Paleogeographic and structural evolution of northwestern Africa and its Atlantic margins since the early Mesozoic. *Geosphere* GES01426.1 (2017) doi:10.1130/GES01426.1.
77. Reyment, R. A. Biogeography of the Saharan Gretaceous and Paleocene epicontinental transgressions. *Cretaceous Research* **1**, 299–327 (1980).
78. Akande, S. O., Ojo, O. J., Erdtmann, B. D. & Hetenyi, M. Paleoenvironments, organic petrology and Rock-Eval studies on source rock facies of the Lower Maastrichtian Patti Formation, southern Bida Basin, Nigeria. *Journal of African Earth Sciences* **41**, 394–406 (2005).
79. Ojo, O. J. & Akande, S. O. Sedimentology and depositional environments of the Maastrichtian Patti Formation, southeastern Bida Basin, Nigeria. *Cretaceous Research* **30**, 1415–1425 (2009).
80. Chardon, D., Grimaud, J.-L., Rouby, D., Beauvais, A. & Christophoul, F. Stabilization of large drainage basins over geological time scales: Cenozoic West Africa, hot spot swell growth, and the Niger River: HOT SPOT SWELL GROWTH AND NIGER RIVER. *Geochem. Geophys. Geosyst.* **17**, 1164–1181 (2016).

81. Friedman, G. M. Distinction between dune, beach and river sands from their textural characteristics. *J Sediment Petrol.* 514–529 (1961).

# Tables

**Table 1:** Recovered palynomorphs from sediments analyzed from the outcrops of the Ise Formation at OB, IJ, ER and OK.

| | OB | | | ER | | | IJ | | | OK | | |
|---|---|---|---|---|---|---|---|---|---|---|---|---|
| | Outcrop samples | | | Outcrop samples | | | Outcrop samples | | | Outcrop samples | | |
| **Palynomorphs** | **1** | **2** | **3** | **1** | **2** | **3** | **1** | **2** | **3** | **1** | **2** | **3** |
| Cyathidites sp. | 1 | - | - | 1 | 1 | | 1 | - | 1 | - | - | - |
| Laevigatosporites sp. | 1 | - | - | - | 1 | 3 | 1 | - | - | 1 | - | 1 |
| Acrostichum aureum | 1 | - | - | - | - | - | - | - | 1 | | - | |
| Fungal spore | 1 | 1 | 1 | - | - | - | 1 | - | - | 1 | - | 1 |
| Monocolpites sp. | 1 | - | - | - | - | - | - | 1 | - | - | - | - |
| Spore indeterminate | - | 1 | - | - | - | - | - | - | - | - | - | - |
| Pollen indeterminate | - | 1 | - | - | - | - | - | - | - | - | - | - |
| Concentricytes sp. | 1 | - | - | - | - | - | - | - | - | - | - | - |
| Trilete spore | - | - | 1 | - | - | - | 1 | - | - | - | - | - |
| Psilatricolporites sp. | - | - | - | 1 | - | - | - | - | - | - | - | - |
| Foveotriletes margaritae | - | - | - | 1 | - | - | 1 | - | - | - | - | - |
| Echitriporites trianguliforms | - | - | - | 1 | - | - | - | 1 | - | - | - | - |
| Verrucatosporites sp. | - | - | - | - | - | 1 | - | - | - | - | - | 1 |
| Monocolpites marginatus | - | - | - | - | - | 1 | 1 | - | - | - | - | - |
| Microforaminiferal wall lining | - | - | - | - | - | 1 | - | - | - | - | - | - |
| Cyathidites minor | - | - | - | - | - | - | 1 | 1 | - | - | 1 | - |
| Longapertites sp. | - | - | - | - | - | - | - | - | 1 | - | - | - |
| Retitricolporites sp. | - | - | - | - | - | - | - | - | 1 | - | - | - |
| Sapotaceae | - | - | - | - | - | - | - | - | 1 | - | 2 | - |
| Spinizonocolpites sp. | - | - | - | - | - | - | - | - | - | 1 | - | - |

# Figures

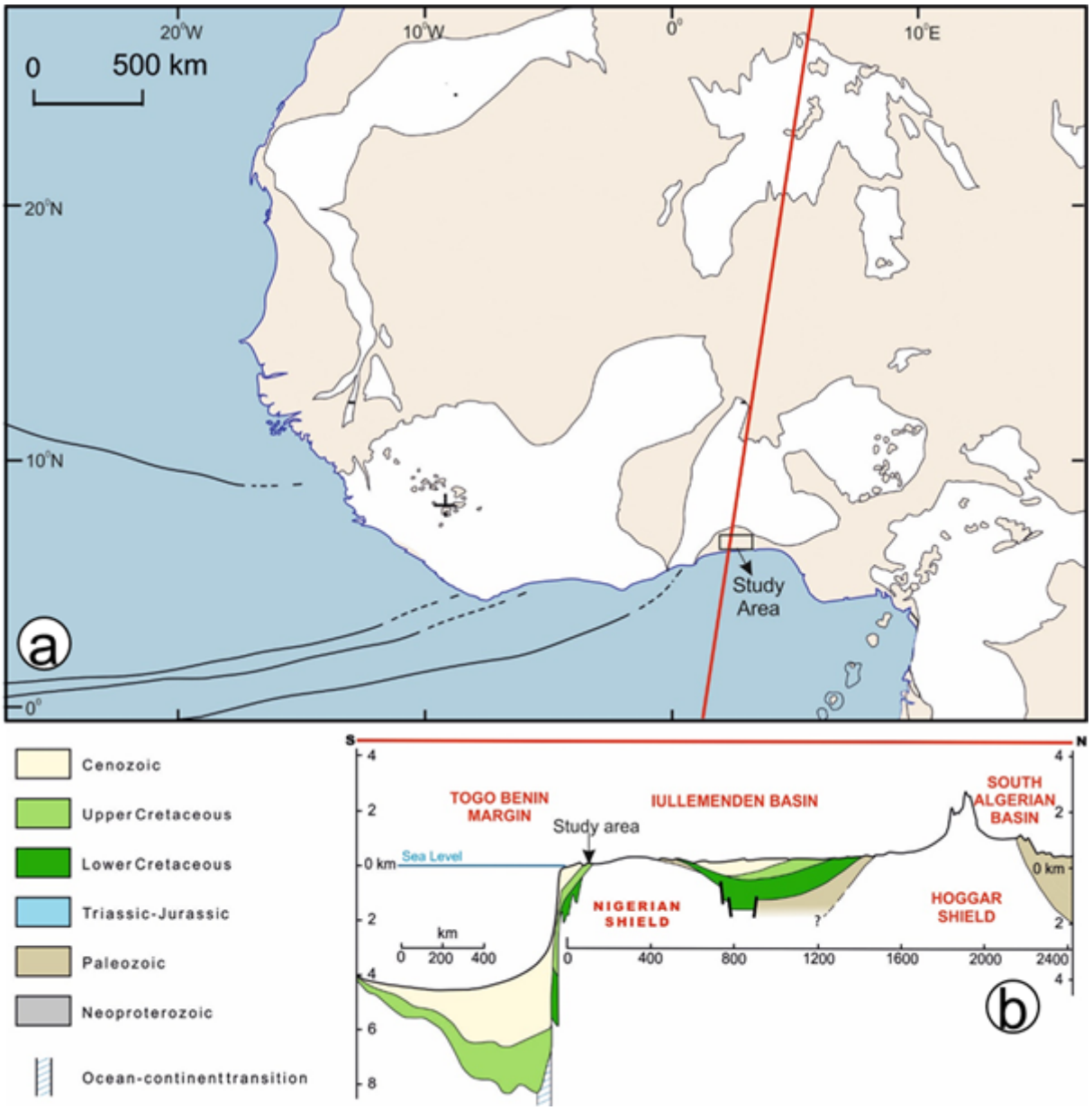


## Figure 1

(a) Map of Central and West Africa showing the rough location of the study area [76]. (b) The transect shows the variation in morphology and rock types from the South Algerian Basin through the Iullemenden Basin and the Togo-Benin Basin. The study area is in the Eastern Dahomey Basin [76].

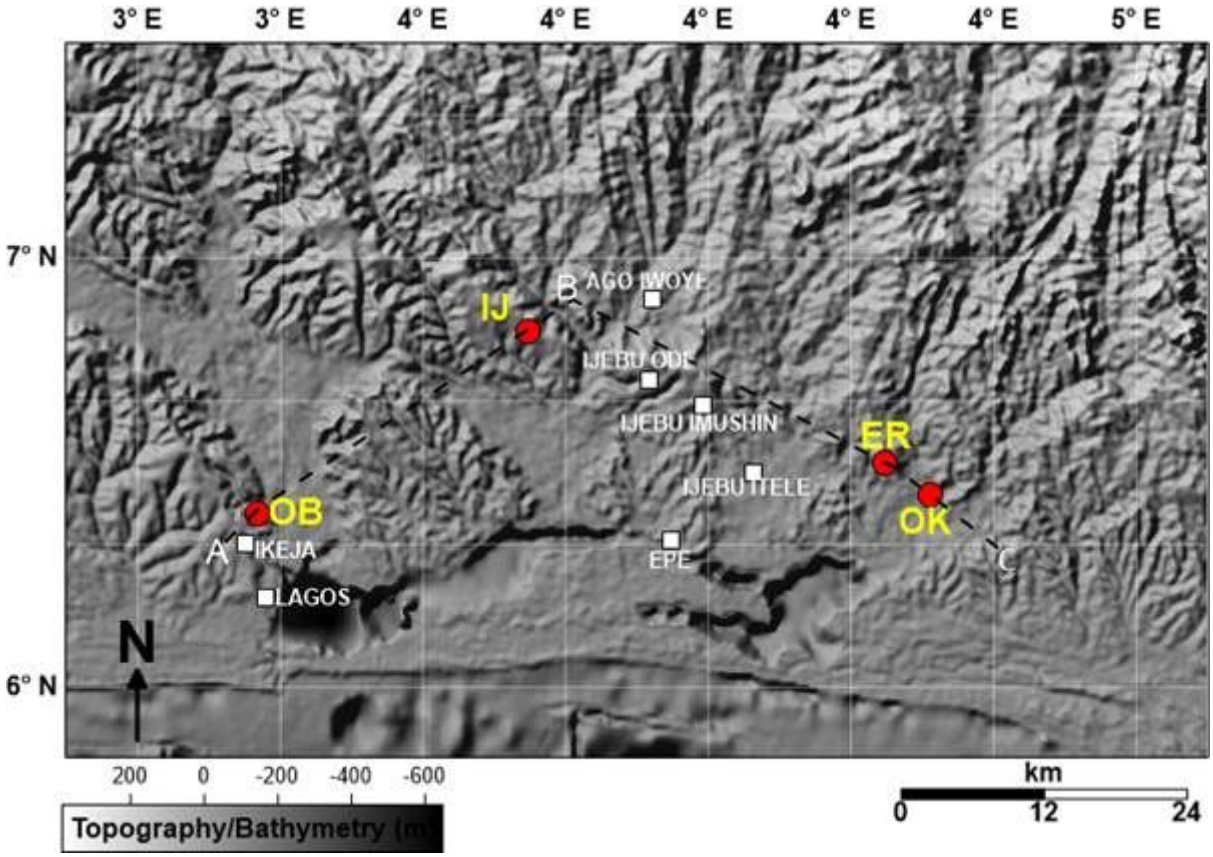


## Figure 2

Topography/bathymetry map of the study area showing the locations of the outcrops. Elevation data was downloaded from GEBCO (https://download.gebco.net/) and gridded in Surfer 16.

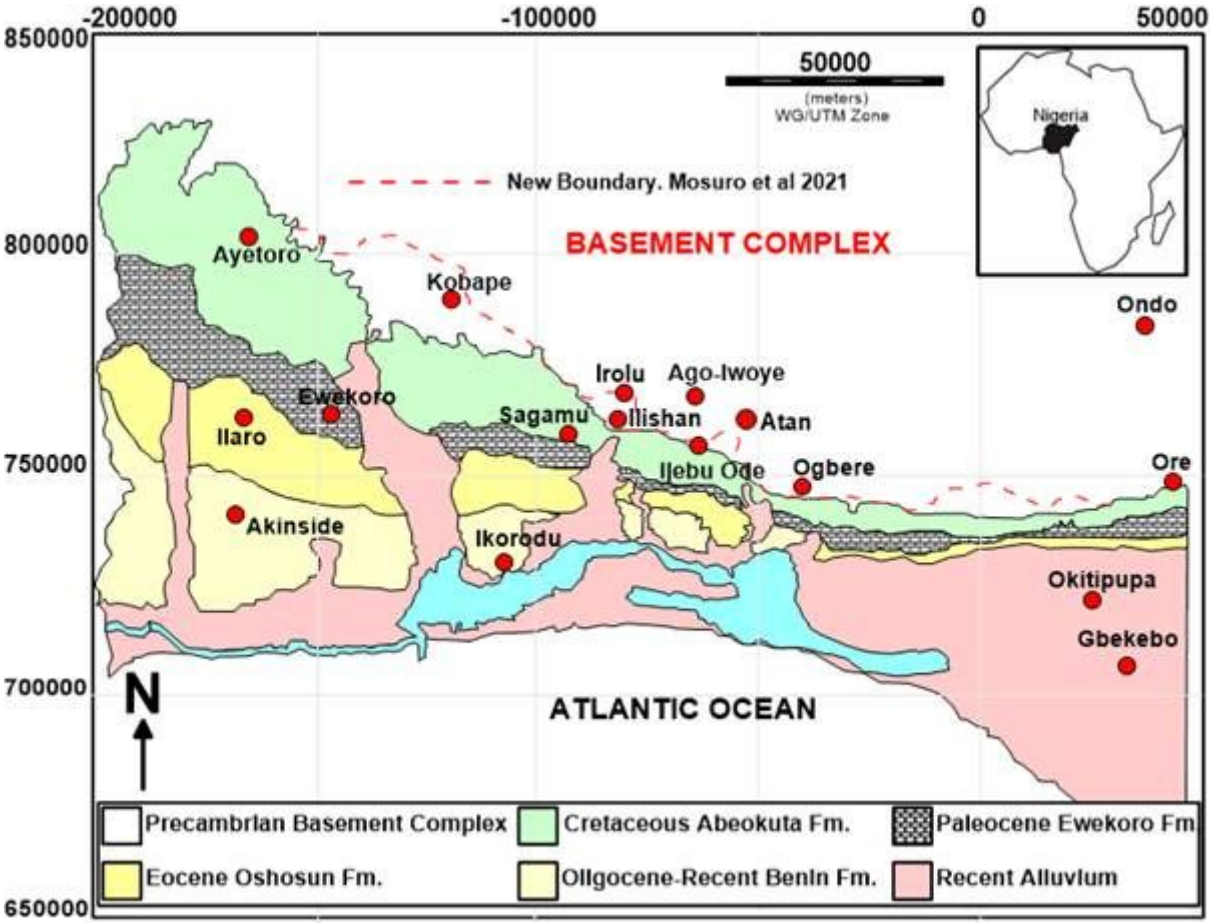


## Figure 3

Redefined geological map of the Eastern Dahomey Basin [4].


## Figure 4

Pictures showing overview of the four outcrops analysed in this work (a) Ojodu Berger, OB (b) Ijebu-Ijesha, IJ, (c) and (d) Eregun, ER and (e) and (f) Onikintigbi, OK. All the outcrops are in the Eastern Dahomey Basin in SW Nigeria.

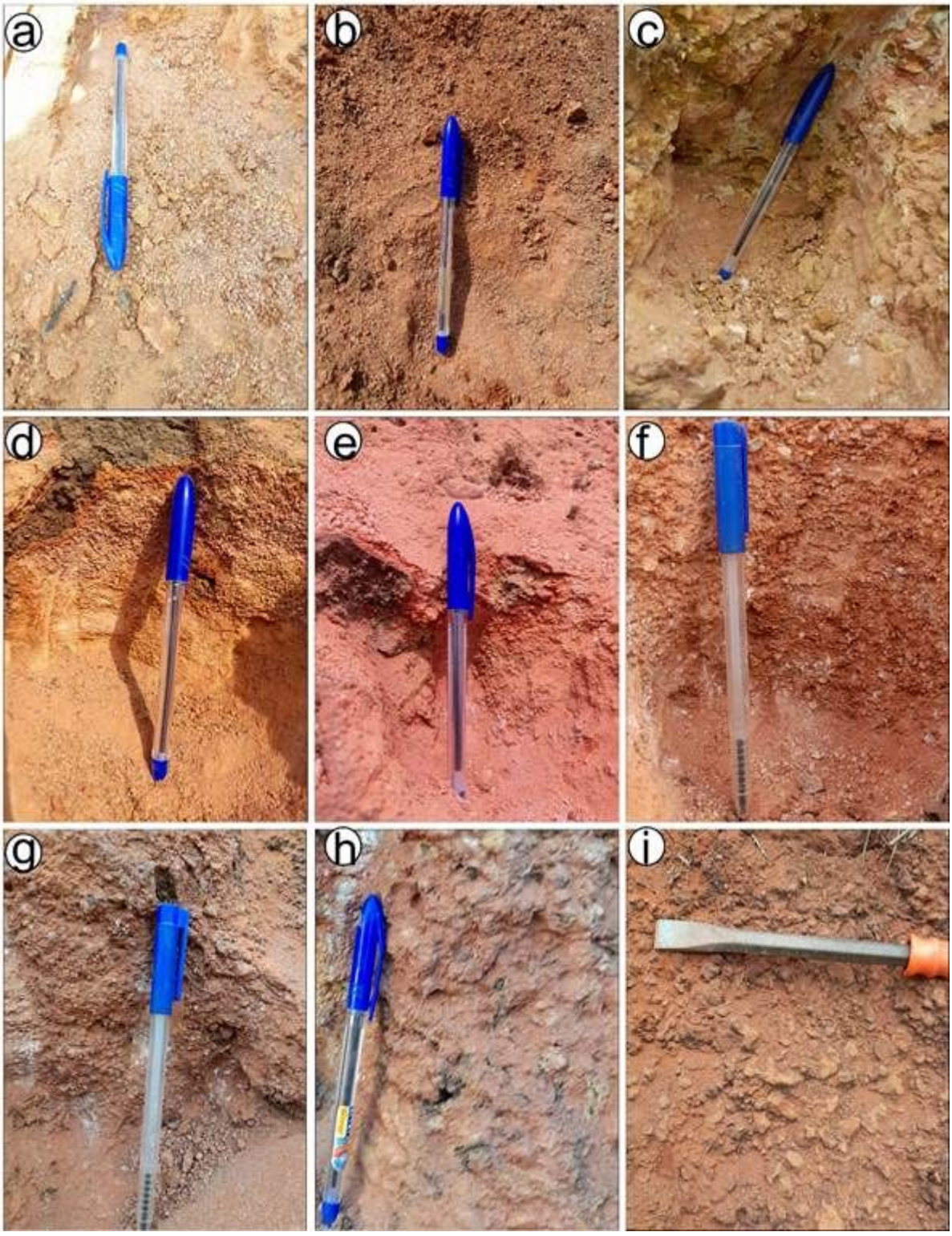


## Figure 5

Lithofacies from some of the outcrop locations (a) coarse-grained sandstone, with a greyish brown color at depth of 2.6 m-3.2 m at OB1, (b) brown to grey, fine to medium grained, clayey sandstone at depth of 3.2 m-3.7 m from OB1 (c) white to light brown and medium to coarse sandstone at depth 0 m-1.3 m at OB3 (d) brownish to yellow, medium to coarse grained sandstone with a clayey feel at the base of log OB1 (e) medium to coarse grained clayey sandstone at 1.3 m-2.7 at OB3 (f) reddish-brown, medium to

coarse-grained sandstone at depth of 0 m-1.8 m at IJ1 (g) brownish to grey, coarse-grained sandstone at 0-1.6 m at IJ3 (h) 0.30 m-0.62 at ER1 (i.) greyish to brown sandstone with subrounded pebbles at 3.2 m-3.6 at IJ1.

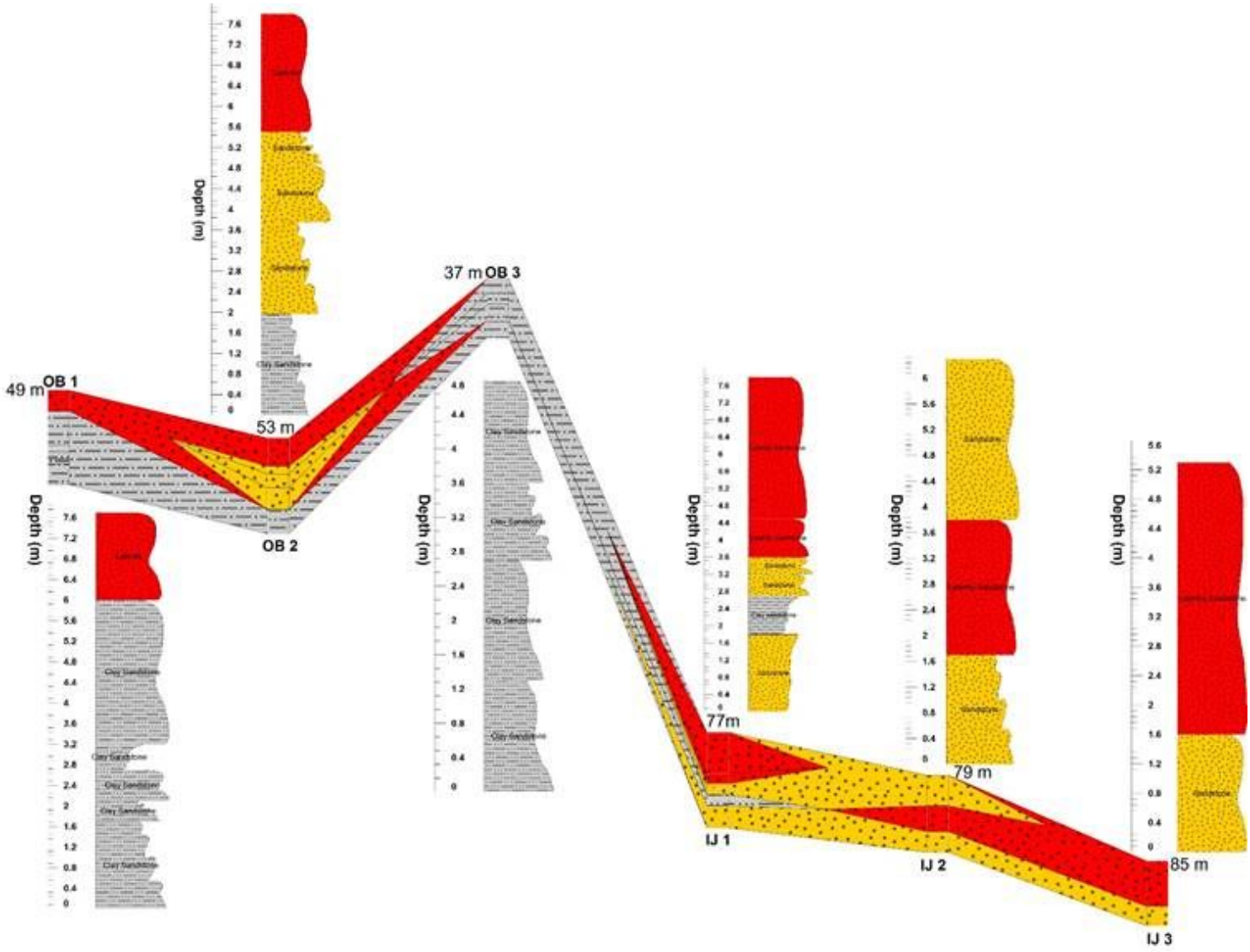


## Figure 6

Correlation panel from OB to IJ showing the regional overview of the Ise Formation. In hand specimen, the sandstones are medium to coarse grained and composed of different clasts. *See location of OB and IJ in Figure 2.*

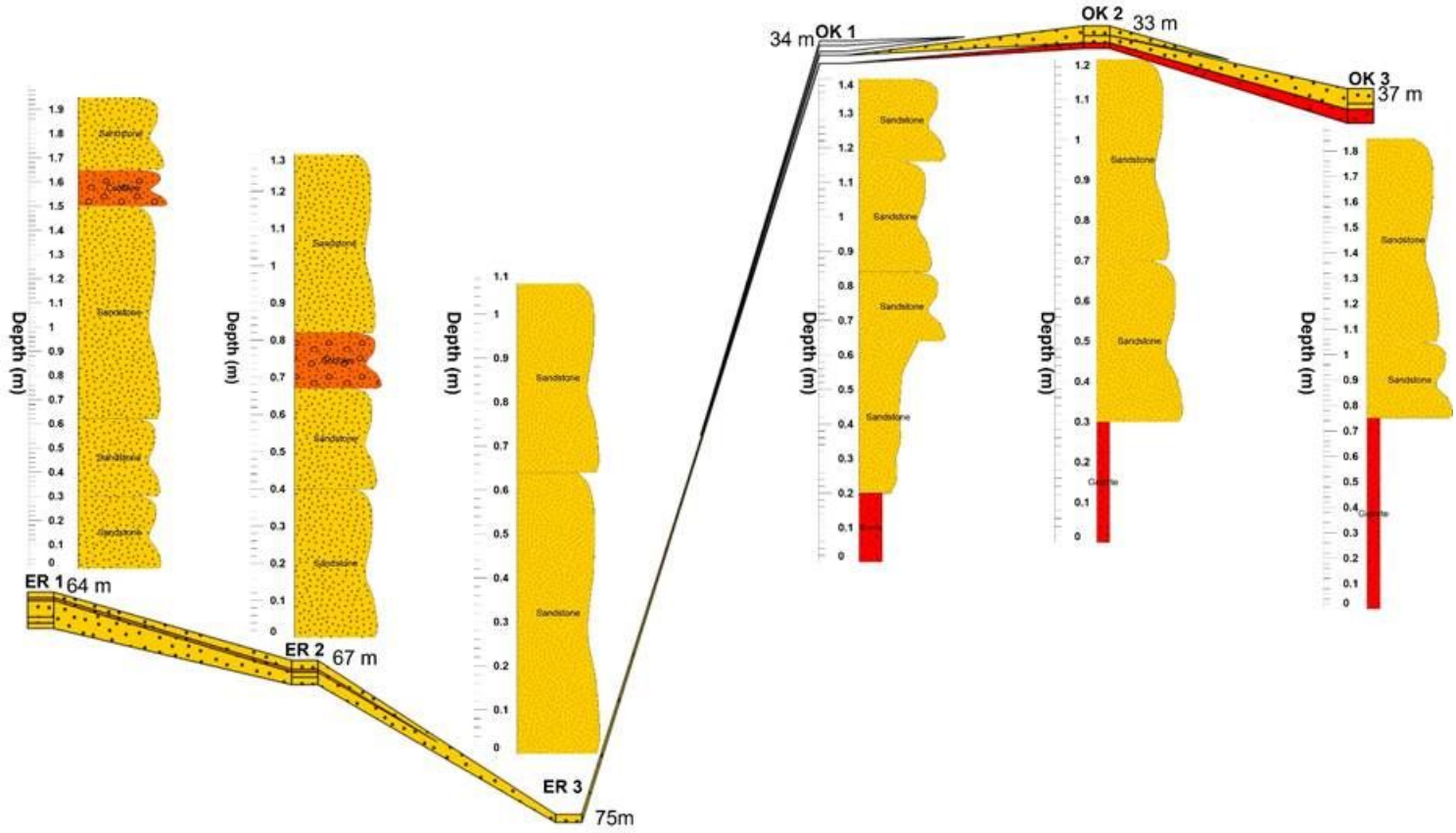


## Figure 7

Correlation panel from ER to OK showing the main lithologic types as logged from the field. The study area is dominated by different sandstone facies. *See location of OB and IJ in Figure 2.*

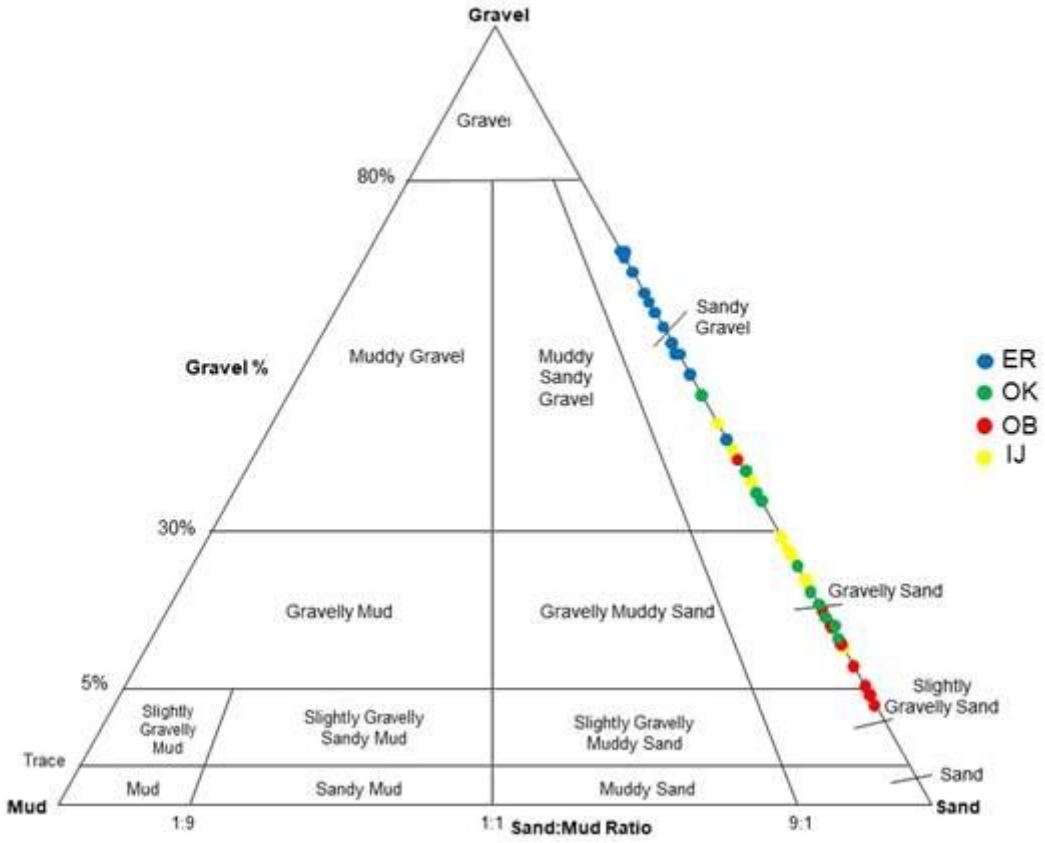


## Figure 8

Ternary plot for characterization of the samples based on their grain distribution. All the samples analyzed at ER are sandy gravels while sediment samples from both OK and IJ overlap between sandy gravel and gravelly sand. The samples from OB include slightly gravelly sands, gravelly sands, and sandy gravels.

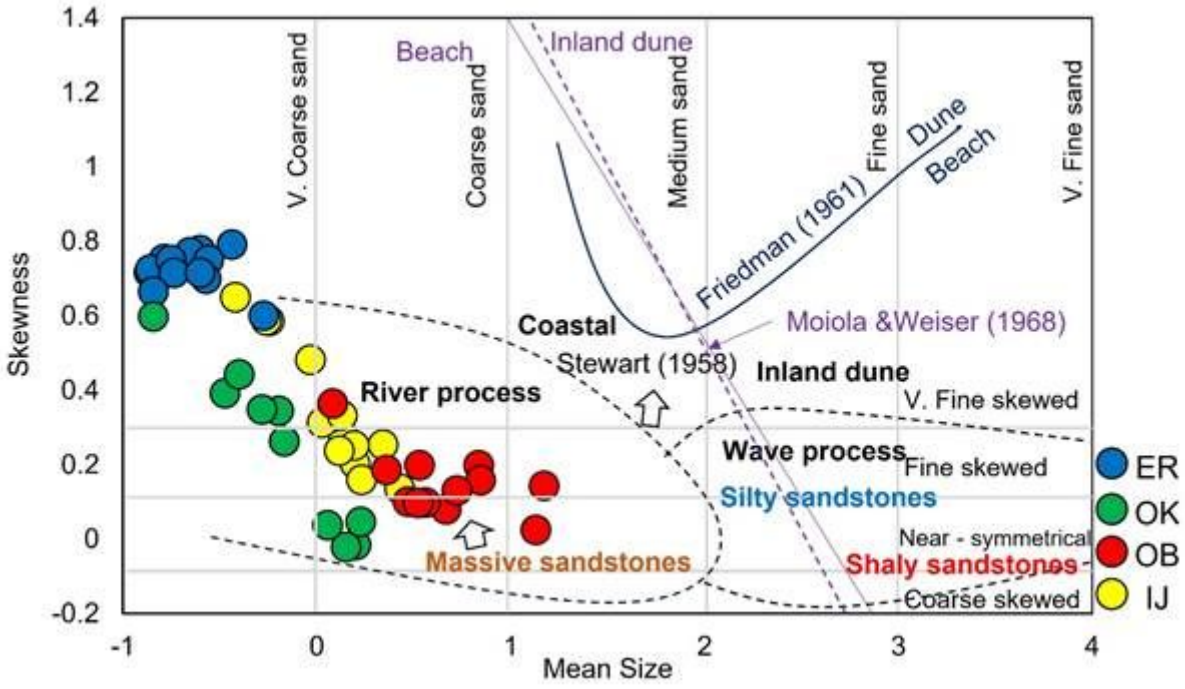


## Figure 9

Bivariate plot of skewness vs mean for ER, OK, OB and IJ showing the different depositional environment, modified after [36,37,81].

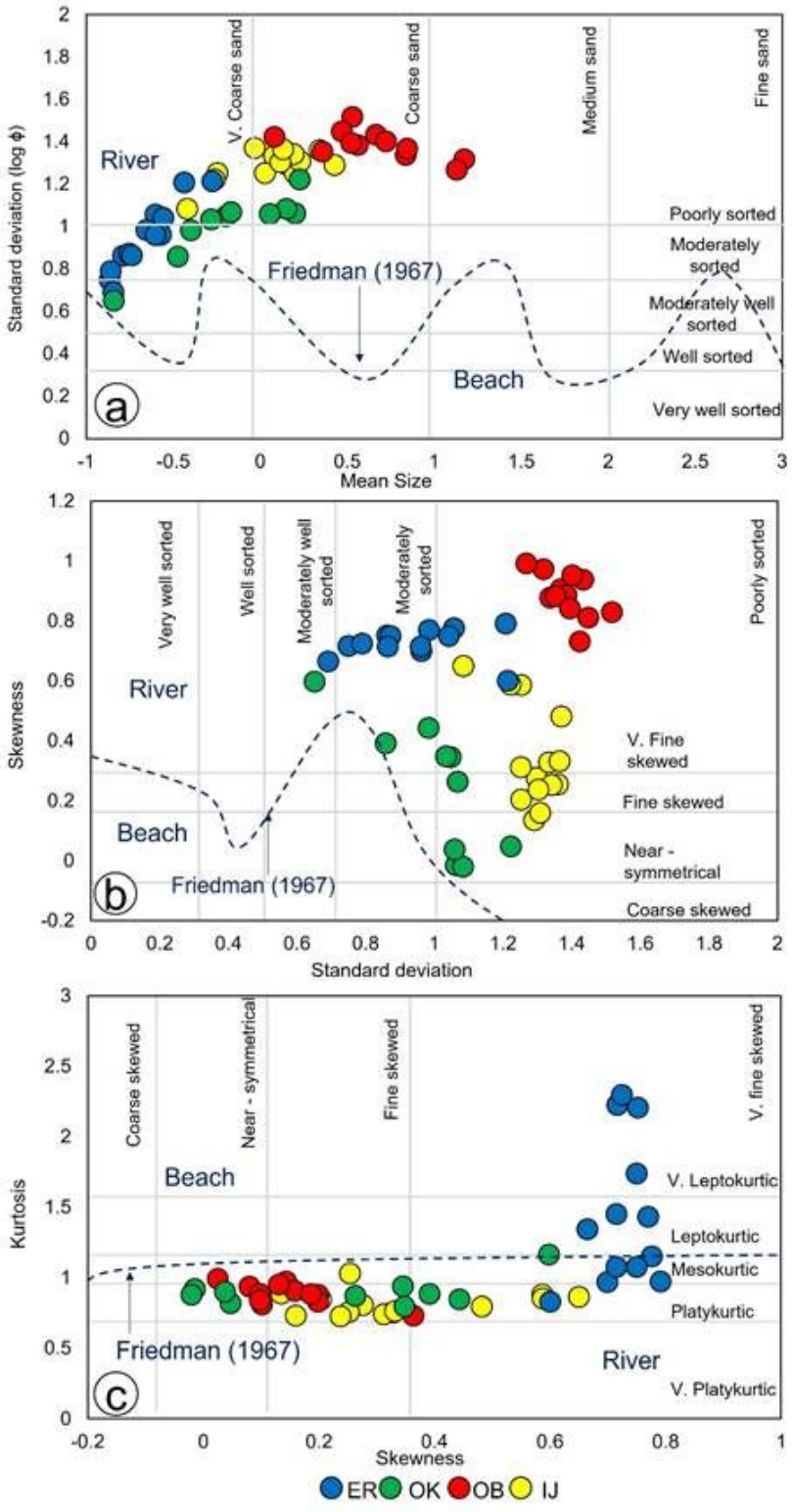


## Figure 10

Bivariate plots for ER, OK, OB and IJ of (a) Standard deviation vs Mean (b) Skewness vs standard deviation and (c) Kurtosis vs skewness. Each showing beach/river environment of deposition. The plots were defined according to the works of [35].

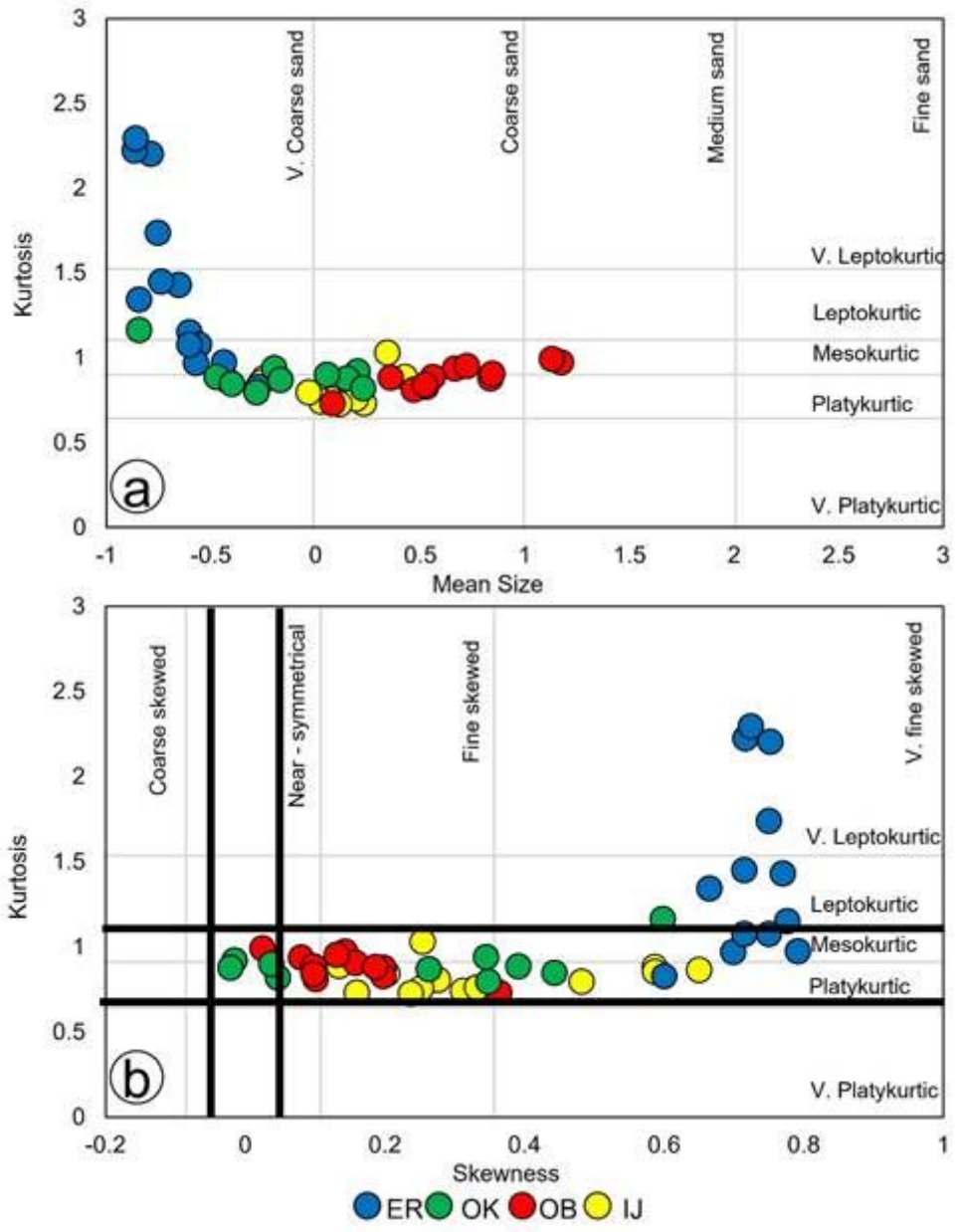


## Figure 11

Bivariate plots for ER, OK, OB and IJ of (a) Kurtosis vs mean size and (b) Kurtosis vs skewness showing the normal trend path and high/low energy domain according to [31].

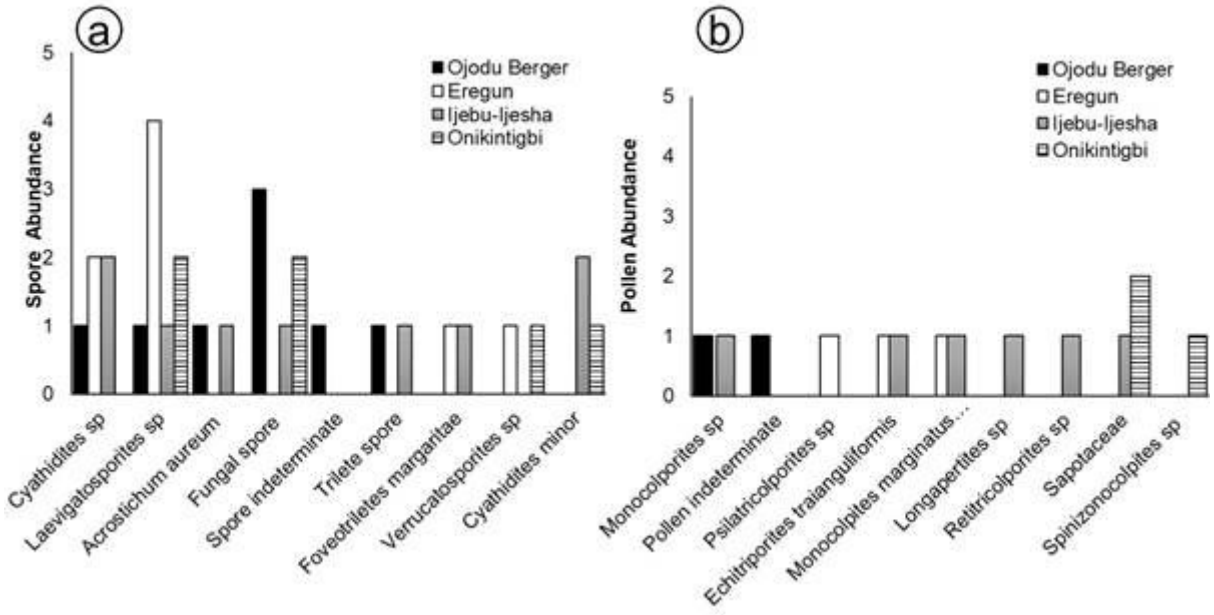


## Figure 12

Histograms showing (a) abundance of spores recovered from the analyzed samples and (b) abundance and types of pollens recovered from the study area.

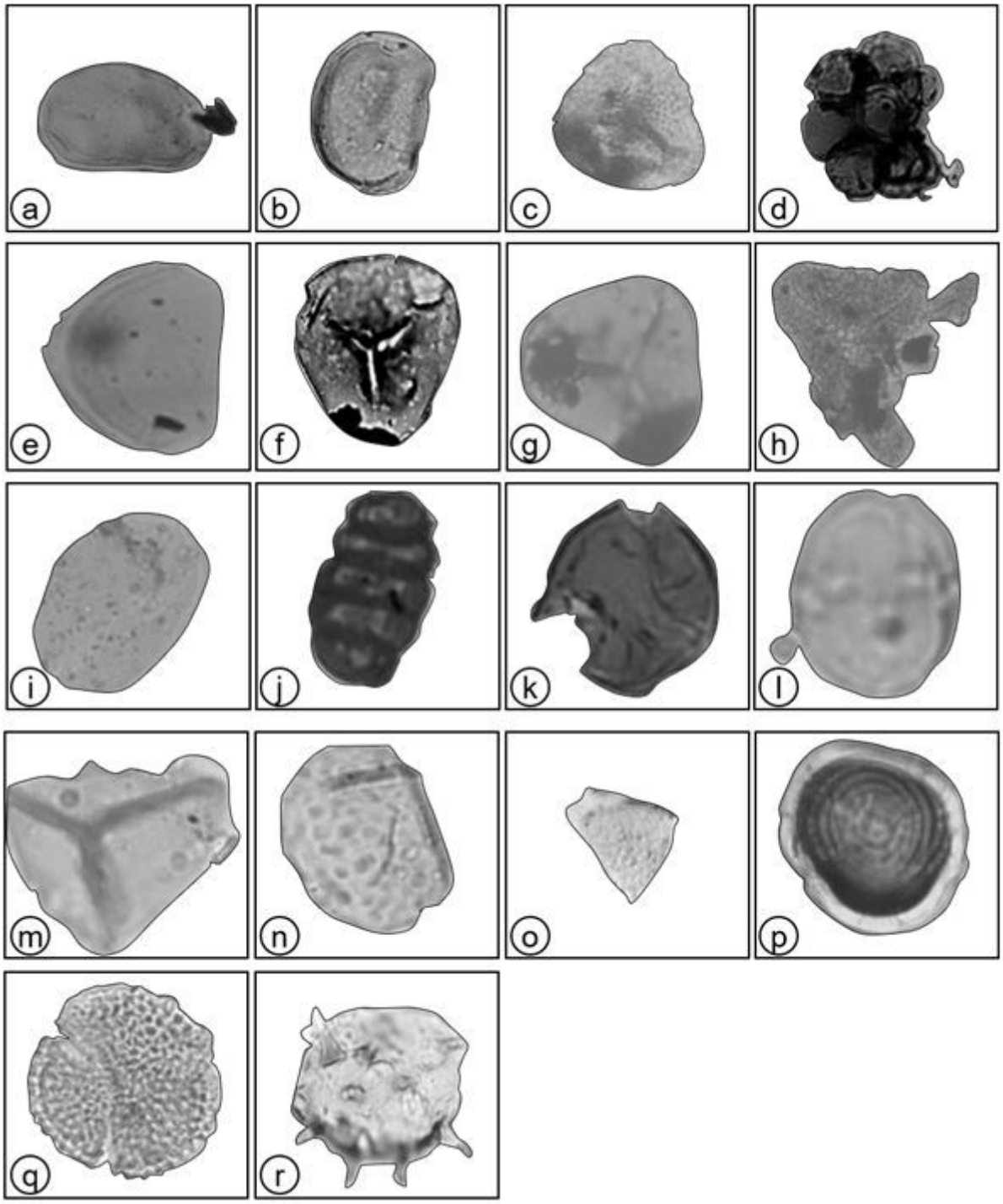


## Figure 13

Photomicrographs of palynomorphs recovered from the study area (a) and (b) Laevigatosporite sp. (c) Foveotriletes margaritae (d) Microforaminiferal wall lining (e) Longapertites sp. (f) Acrostichum aureum (g) Cyathidites minor (h) Cyathidites sp. (i) Monocolpites marginatus (j) Fungal Spore (k) Psilatricolporites sp. (l) Sapotaceae sp. (m) Trilete Spore (n) Verrucatosporite sp. (o) Echitriporites trianguliforms (p) Concentricytes sp (q) Retitricolpites sp. (r) Spinizonocolpites sp.

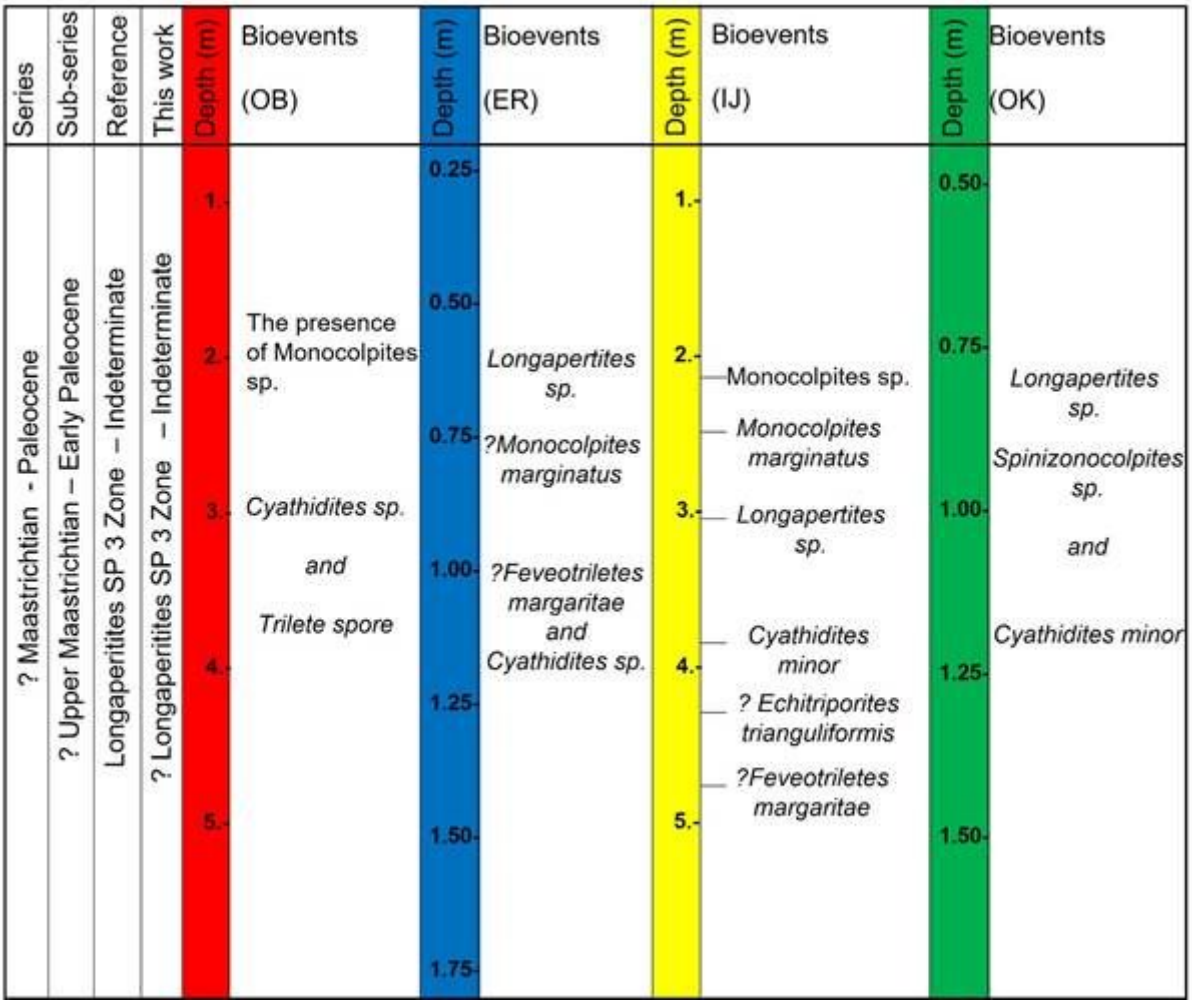


## Figure 14

Palynomorphs assemblages and biodiversity has recovered from the 50 samples analyzed in the study area. Based on the palynomorph assemblages an age of Upper Maastrichtian is assigned to the Ise Formation.

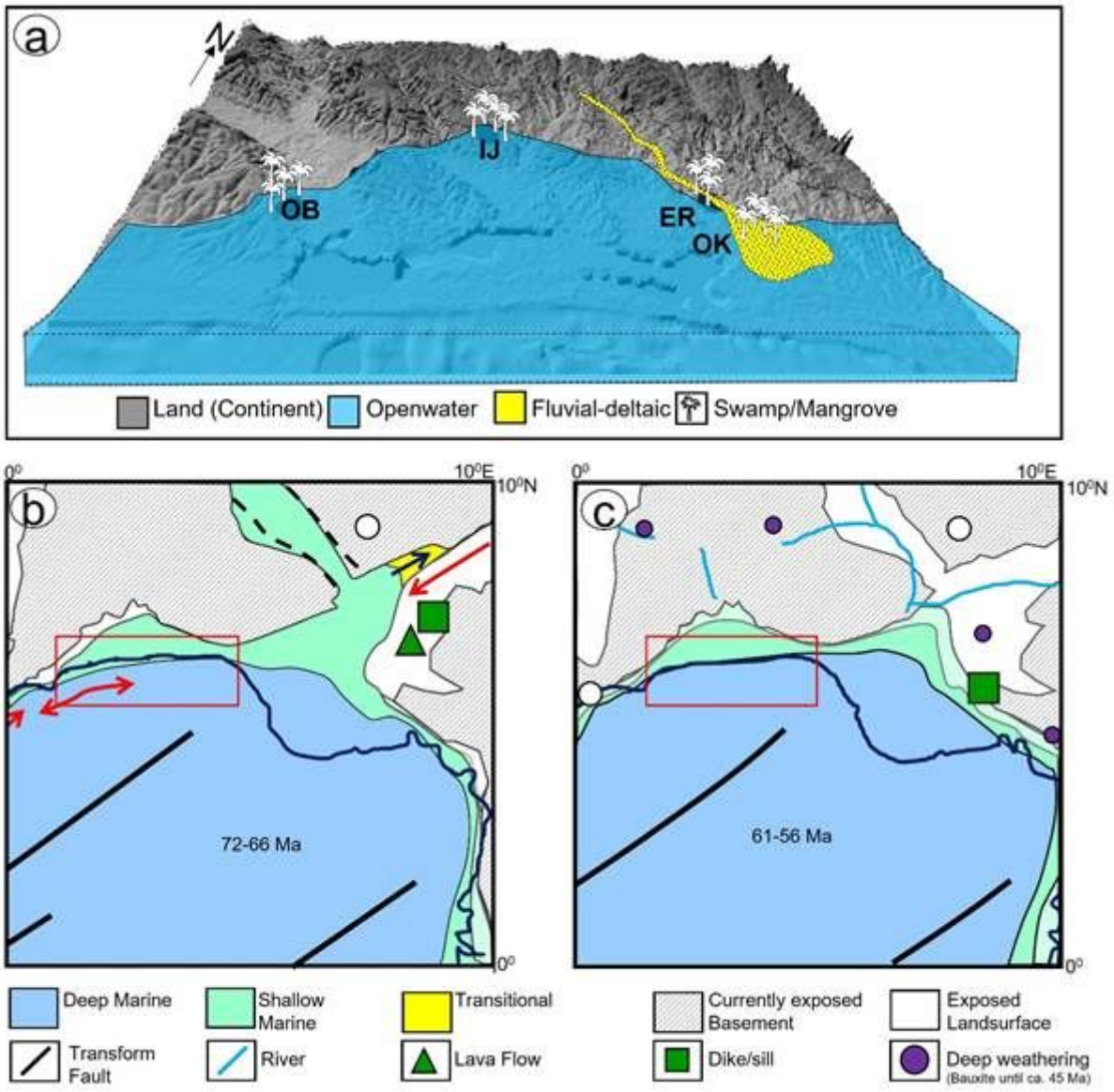


**Figure 15**

(a) Conceptual model showing the depositional environment of the Ise Formation in Eastern Dahomey Basin. The top map is the 3D view of the present-day elevation profile of the study area from Figure 2. Geological configuration of Nigeria and Southern Atlantic Ocean during the (b) Maastrichtian, 72-66 Ma and (c) Late Paleocene, 61-56 Ma (Modified from [76]. *Note: Location of the present-day Eastern Dahomey Basin is marked with red rectangle.*

# Supplementary Files

This is a list of supplementary files associated with this preprint. Click to download.

- Grainsizeanalysisdata.xlsx